SYNTHESIS OF PARACYCLOPHANE-PEPTIDE BASED SEMI-CONDUCTIVE PEPTIDE HYDROGELS

A THESIS SUBMITTED TO
THE GRADUATE SCHOOL OF NATURAL AND APPLIED SCIENCES
OF
MIDDLE EAST TECHNICAL UNIVERSITY

BY

VOLKAN DOLGUN

IN PARTIAL FULFILLMENT OF THE REQUIREMENTS
FOR
THE DEGREE OF MASTER OF SCIENCE
IN
CHEMISTRY

SEPTEMBER 2017

Approval of the thesis

SYNTHESIS OF PARACYCLOPHANE-PEPTIDE BASED SEMI-CONDUCTIVE PEPTIDE HYDROGELS

submitted by **VOLKAN DOLGUN** in partial fulfillment of the requirements for the degree of **Master of Science in Chemistry Department, Middle East Technical University** by,

Prof. Dr. Gülbin Dural Ünver
Dean, Graduate School of **Natural and Applied Sciences** _____

Prof. Dr. Cihangir Tanyeli
Head of Department, **Chemistry** _____

Assist. Prof. Dr. Salih Özçubukçu
Supervisor, **Department of Chemistry, METU** _____

Examining Committee Members:

Prof. Dr. Metin Zora _____
Department of Chemistry, METU

Assist. Prof. Dr. Salih Özçubukçu _____
Department of Chemistry, METU

Assist. Prof. Dr. Yunus Emre Türkmen _____
Department of Chemistry, Bilkent University

Assist. Prof. Dr. Emrullah Görkem Günbaş _____
Department of Chemistry, METU

Assist. Prof. Dr. Rükan Genç _____
Department of Chemical Engineering, Mersin University

Date: 07.09.2017

I hereby declare that all information in this document has been obtained and presented in accordance with academic rules and ethical conduct. I also declare that, as required by these rules and conduct, I have fully cited and referenced all material and results that are not original to this work.

Name, Last name: Volkan Dolgun

Signature:

ABSTRACT

SYNTHESIS OF PARACYCLOPHANE-PEPTIDE BASED SEMI-CONDUCTIVE PEPTIDE HYDROGELS

Dolgun, Volkan

M.Sc., Department of Chemistry
Supervisor: Assist. Prof. Dr. Salih Özçubukçu

September 2017, 73 pages

Self-assembling peptide hydrogels are becoming an emerging field especially in last decades. Application of these hydrogel forming peptides in biomedical materials, organic electronic devices and tissue engineering is a challenging topic which requires alternative structures to get better and to be easily applied systems. [2.2]Paracyclophane has an interesting structure which two benzene rings are bound to each other with a bridge containing 2 carbons. It is known that the distance between two benzene rings of paracyclophane is shorter, 2.8 - 3.1 Å, than the optimum pi-pi stacking. This provides an easier electron transfer between two rings and makes the compound conductive. On this work, ferrocenoyl phenylalanine (**FF**) was synthesized and semi-conductive hydrogels were obtained. Electrical properties of these hydrogels such as dielectric constants, conductivities, mobilities and conductivity mechanisms were extensively studied. Organic field-effect transistor which requires low voltage and power was also developed using **FF** hydrogels. In the second part of the work, three [2.2]paracyclophane mono amino acid and nine dipeptide derivatives were

synthesized and characterized by spectroscopic methods. However, it was failed to form hydrogels from these peptide derivatives under various conditions. [2.2]paracyclophane-2-carboxylic was resolved into its enantiomers using chiral amine. Enantiopure [2.2]Paracyclophanoyl phenylalanine was synthesized using each enantiomer of [2.2]paracyclophane-2-carboxylic acid. Hydrogelation studies have not been completed yet.

Keywords: [2.2]paracyclophane, ferrocene, peptide hydrogel, self-assembly, semi-conductors.

ÖZ

PARASİKLOFAN-PEPTİT BAZLI YARI-İLETKEN PEPTİT HİDROJEL SENTEZİ

Dolgun, Volkan

Yüksek Lisans, Kimya Bölümü
Tez Yöneticisi: Yrd. Doç. Dr. Salih Özçubukçu

Eylül 2017, 73 sayfa

Kendiliğinden yapılanan peptit hidrojeller özellikle son yıllarda gelişen bir çalışma alanı olmuştur. Hidrojel oluşturabilen bu peptitlerin doku mühendisliği, organik elektronik ve biyomedikal malzelemelerde kullanımı, alternatif yapılar gerektiren zor bir konudur. [2.2]Parasiklofan, iki adet benzen halkasının iki karbonlu köprü ile birbirine bağlandığı ilginç geometriye sahip bir moleküldür. Parasiklofanın iki benzene halkası arasındaki mesafe optimum pi-pi istiflenmesinden daha kısa olarak 2,8-3,1 Å olduğu bilinmektedir. Bu da iki halka arasındaki elektron transferinin daha kolay olmasını iletkenlik göstermesini sağlamaktadır. Bu çalışmada, ferrosenil fenilalanin (**FF**) sentezlenmiş ve bu yapıdan yarı-iletken hidrojeller elde edilmiştir. Bu hidrojellerin, dielektrik sabitleri, iletkenlikleri, mobiliteleri ve iletkenlik mekanizmaları gibi elektriksel özellikleri kapsamlı olarak incelenmiştir. **FF** hidrojelleri kullanılarak düşük voltaj ve güç gerektiren organik alan etkili transistör geliştirilmiştir. Çalışmanın ikinci kısmında, üç [2,2]parasiklofan mono amino asit ve 9 dipeptit türevleri sentezlenmiş ve spektroskopik yöntemlerle karakterize edilmiştir. Ancak, çeşitli parametreler denenmesine rağmen bu peptit türevlerinden hidrojel elde edilememiştir.

[2,2]Parasiklofan-2-karbokslik asit, kiral amin kullanılarak enantiyomerlerine ayrılmıştır. Her iki enantiyomer de kullanılarak enantiyosaf [2,2]parasiklofanil fenilalaninler sentezlenmiştir ama hidrojel çalışmaları henüz tamamlanmamıştır.

Anahtar Kelimeler: [2.2]parasiklofan, ferrosen, peptit hidrojeller, kendiliğinden yapılanma, yarı-iletkenlik

To everything that made me who I am today

ACKNOWLEDGEMENTS

I would like to express my genuine gratitude to my supervisor Assist. Prof. Dr. Salih Özçubukçu for his precious guidance and encouragement. It would have been impossible for me to conclude this work without his endless patience and invaluable advices. It has been a great honor for me to be a part of his research group as a graduate student.

I also would like to thank every single member of Özçubukçu Research group, Mehmet Seçkin Kesici, Muzaffer Gökçe, Dr. Aytül Saylam, Orkun Evran, Melek Parlak, Güzide Aykent, Tuğçe Yılmaz and Burcu Okyar for their precious friendship, advices and helps.

I also would like to thank Çiğdem Çakırlar and Prof. Dr. Sait Eren San for the investigation of electrical properties of hydrogels.

I wish to thank NMR specialist Betül Eymur for NMR analysis in our department and Elif Kanbertay Canlı for HRMS analysis in central laboratory of METU.

I would like to thank TUBİTAK (115Z730) and BAP for financial support.

I wish to express my gratitude to the academic stuff of Department of Chemistry at METU for their supports and guidance throughout my whole undergraduate and graduate years.

A special thanks to my friend Hakan Güner and my cousin Hakan Dolgun for their priceless friendships

Finally, I would thank my family for their endless love.

TABLE OF CONTENTS

LIST OF TABLES

TABLES

LIST OF FIGURES

FIGURES

LIST OF SCHEMES

SCHEMES

LIST OF ABBREVIATIONS

DCM : Dichloromethane

DIEA : N,N-Diisopropylethylamine

DMF : N,N-Dimethylformamide

DMSO : Dimethyl sulfoxide

FMOC : Fluorenylmethyloxycarbonyl

HBTU : 2-(1H-Benzotriazole-1-yl)-1,1,3,3-tetramethyluronium hexafluorophosphate

HOBt : Hydroxybenzotriazole

HPLC : High performance liquid chromatography

HRMS : High-resolution mass spectrometry

NMR : Nuclear magnetic resonance spectroscopy

OFET : Organic field-effect transistor

SPPS : Solid phase peptide synthesis

TFA : Trifluoroacetic acid

TLC : Thin layer chromatography

TMS : Trimethylsilane

CHAPTER 1

INTRODUCTION

1.1 Self-assembly

Self-assembly is about the simultaneous association of many single terms into a systematic arrangement and, well-ordered structures to enhance the interest of the individual without external intervention [1]. Molecular self-assembly, widely used in nanotechnology, molecules' or ions' spontaneous association to structure more organized and larger forms with the construction of reversible interactions [2]. Combination of variable non-covalent communications is required to form these well-organized and ordered structures. These are individually rather weak, such as hydrophobicity, van der Waals and hydrogen bond interactions. Though, overall combination of those interactions can produce highly stable structures. However, under specific reaction conditions, one component will be the superior over the all combinations because of its thermodynamic stability. For this reason, in formation of structures, self-assembly is considered as thermodynamically selective [3].

1.1.1 Self-assembly of peptides

For generating chemical compounds which have many different physical and chemical properties, molecular self-assembly is a very effective method [4]. After fortuitous discovery in yeast from the self-assembly of ionic self-complementary

peptides [5], designing peptide systems having self-assembly is accelerated as it is shown in Table 1. Particularly β-sheet forming peptides establish great capability to self-assemble into 1D nanostructure [1].

Table 1. Examples of self-assembled peptides [1].

Name	Sequence	Charge Distribution	Structure
KLE12-I	KLELKLELKLEL	+ - + - + -	β – sheet
RAD16-IV	RARARARADADADADA	+ + + + - - - -	β – sheet
DAR32-IV	DADADADARARARARA	- - - - + + + +	β – sheet and α- helix
RADA16-I	RADARADARADARADA	+ - + - + - + -	β – sheet
EAKA16-I	AEAKAEAKAEAKAEAK	- + - + - + - +	β – sheet
EFK12-I	FEFKFEFKFEFK	- + - + - +	β – sheet

1.2 Peptide hydrogels

The first definition of gel was given by Thomas Graham in 1861 that "*while the rigidity of the crystalline structure shuts out external expressions, the softness of the gelatinous colloid partakes of fluidity and enables the colloid to become a medium for liquid diffusion, like water itself*." [6]. The general definition can be said that when a pot of gel is turned to upside down it is able to maintain its weight without falling which is called inversion test. In 1974, Flory defined gel as "*a gel has a continuous structure that is permanent on the analytical time scale and is solid-like in its rheological behavior.*" [7]

There are mainly four type of gel depending on their constituents: Hydrogel, organogels, xerogel and aerogel. A hydrogel is made of a gelator and water. Similarly, organogels is made of a gelator and an organic solvent. Xerogel is the solid that formed after a hydrogel or organogels is dried completely. Aerogel is the solid formed after

solvent removal under special conditions which does not cause shrinkage so that the material will be very porous [8].

Peptide hydrogels have been under intense scrutiny in recent years due to its potential applications in tissue engineering, selective drug release and biomedical fields [9]. The diversity of the amino acids that make up the peptides provides an excellent opportunity to obtain peptide constructs with variable physical and chemical properties. In addition to 21 natural amino acids (including selenocysteine), it is possible to obtain different properties by using unnatural, synthetic amino acids which offers different applications. Due to the fertility of the peptide chemistry, the interest shown in hydrogel-forming peptides is increasing every year. However, the production of biomaterials for application from such hydrogels based on peptides is a challenging field for many researchers. For example, in 2008 Ulijn, [10] achieved to obtain hydrogel of N-fluorenylmethoxycarbonyl di-phenylalanine (Fmoc-FF) using self-assembly (Figure 1).

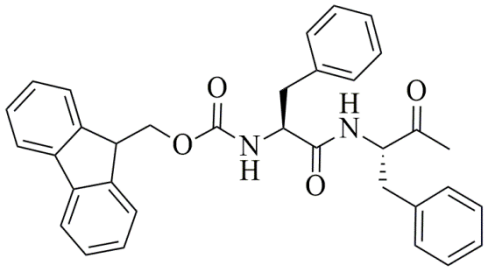

Figure 1. Molecular structure of Fmoc-FF [10].

1.2.1 Peptide-based conductive hydrogels

Peptide-based conductive hydrogel studies are rather new topic in the literature. In recent times, there are few researchers working for the same purpose. These researchers often use beta-sheet forming peptides to design hydrogels. However, due to the long distance (approximately 4.7-5.0 Å), only low conductivities have been obtained. For example, Tovar [11] (Figure 2) and Stupp [12] studied independently that self-assembled thiophene group which is attached between two

peptide sequences contributed to beta-sheet formation. Despite the fact that they proved with spectroscopic methods that there is an electronical connection between π-conjugated thiophene groups because of the self-assembly, they did not measure the conductivities of these structures.

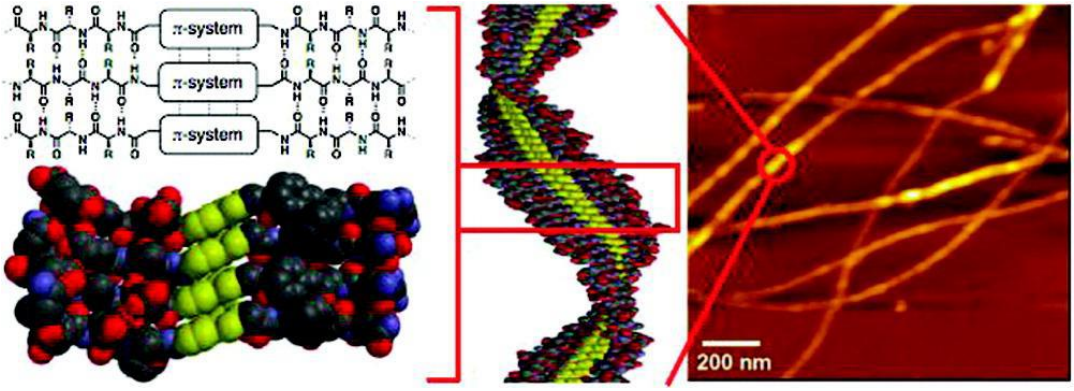

Figure 2. Tovar's peptide hydrogels [11]. Copyright © 2008 American Chemical Society. Adapted with permission.

In 2011, Stupp [12] synthesized another peptide derivatives contained thiophene groups and obtained self-assembled organogels with hydrogen bonding. As a result of this study, Stupp pointed out that melting point of quinquethiophene derivatives were higher than quarterthiophene derivatives (Figure 3). That indicates that increasing the conjugated thiophene groups provides better π-π stacking and better thermal stability. Stupp also investigated the conductivity of these organogels. With the measurements with 4-point probe configuration, the conductivity was measured as $9 \pm 1.7\times10^{-6}$ $S.cm^{-1}$. In this way, it is proved that aromatic groups provide semi-conductivity as a result of π-π stacking.

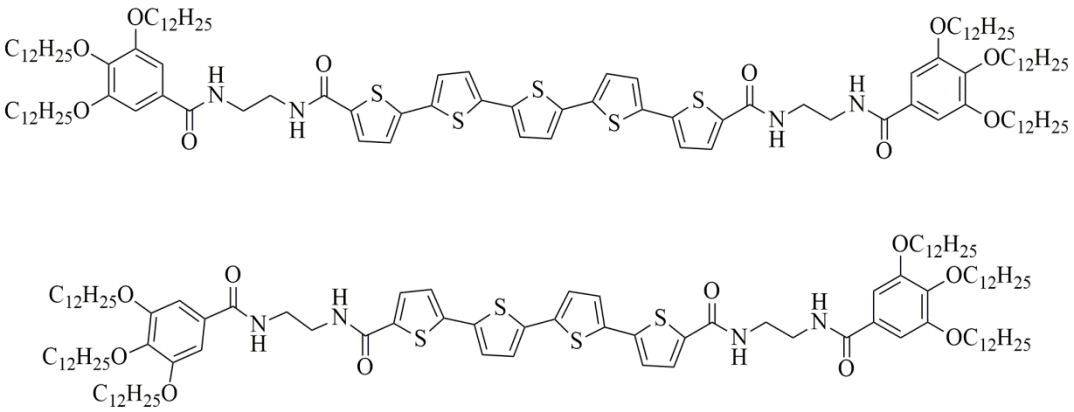

Figure 3 Quinquethiophene and quarterthiophene derivatives [12].

In 2010, Ulijn [14] demonstrated that small peptides containing Fmoc group were able to form beta-sheet with self-assembly (Figure 4). The distance between Fmoc groups were calculated theoretically as 3.6-3.8 Å and resistance in vacuum and air was calculated 0.1 MΩ/sq and 500 MΩ/sq respectively.

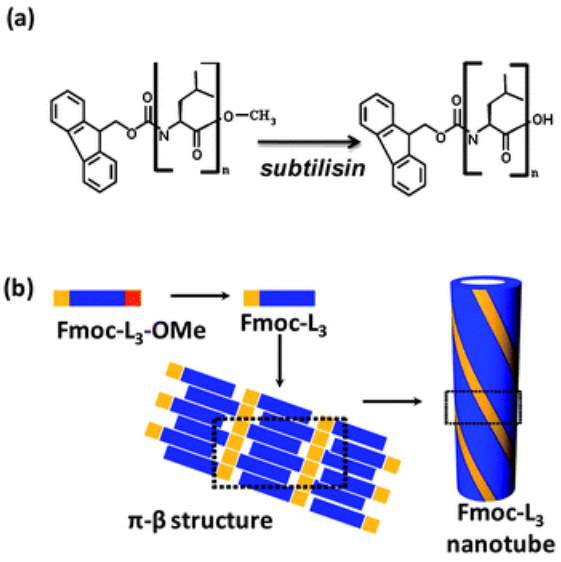

Figure 4. Ulijn's peptide conductive nanotubes [14]. Copyright © 2010 Chemical Society Reviews. Adapted with permission.

In 2011, Tovar [15] achieved to obtain peptide hydrogels having better conductivity. They designed the self-assembly of peptides in two dimension. Instead of the diagonal and complex nanofiber structure, they constructed peptide hydrogels arranged in a single direction and obtained hydrogels which were able to be used in organic electronic applications (Figure 5).

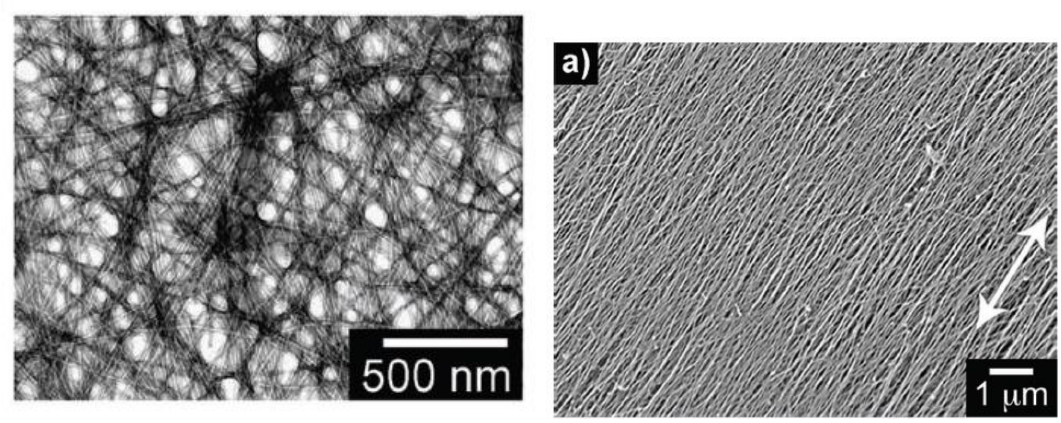

Figure 5. TEM images of regular and self-assembled in one direction peptide hydrogels [15].

1.3 Low-molecular weight hydrogels

Since the publication of hydrogelation of dibenzoyl cysteine by Brenzinger in 1892 [16], it is known that low molecular weight (LMW) molecules can be used as hydrogelators. After a few serendipitous discovers, designed LMW molecules which capable of gel in aqueous solutions has been shown great interest over past decades [17]. LMW hydrogelators generally consist of either long hydrocarbon chain or aromatic groups which provide hydrophobicity to ensure self-assembly in water and a hydrophilic part to establish water compatibility. Being easily prepared and being usable of biocompatitive materials, such as L-amino acids, have drawn attention of scientists. Tiller [18] designed the first drug which able to form hydrogel deriving the antibiotic vancomycin with a pyrene. Another study of using LMW molecules as hydrogelators that with the presence of Na_2CO_3, Xu and co-workers [19] hydrogelated the combination of two Fmoc-protected amino acids (Figure 6) and reported that it can be used as drugs.

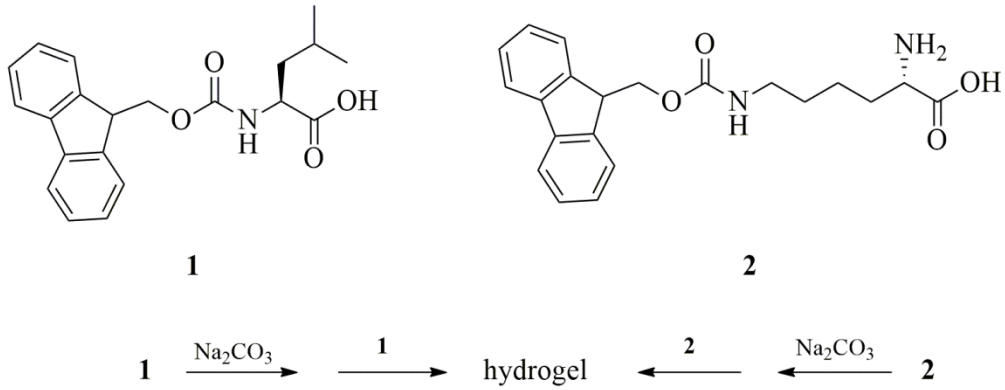

Figure 6. Molecular structures of two amino acids Xu used as hydrogelators [16].

1.3.1 Ferrocenoyl phenylalanine

As it has been mentioned in the section 1.4 low molecular weight hydrogelling agents have been the center of the many researches because of their potential ability. Thanks to another serendipitous discovery in 2013 by Zhang's group [20], not only a remarkably simple hydrogelator but also the lowest molecular weight molecule which can form hydrogel was proposed. Ferrocenoyl molecules are used as organogelators by many researchers [21, 22] because of its aromatic π-π interaction. Zhang and co-workers turned an organogelating agent to hydrogelator by attaching a single aromatic amino acid (phenylalanine) to ferrocene molecule (FF hydrogel). They also tried to make hydrogel of ferrocenoyl tyrosine and ferrocenoyl tryptophan but could not observe any hydrogelation. They published atomic force microscopy (AFM), scanning electron microscopy (SEM) and transmission electron microscopy (TEM) images (Figure 7) of FF hydrogels and made density functional theory (DFT) calculations but did not investigate its electrical properties.

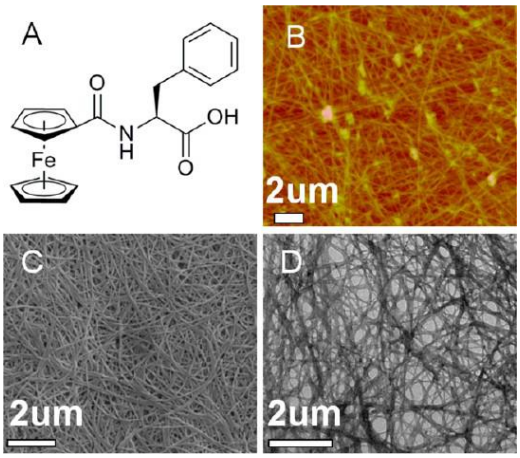

Figure 7. (A) Ferrocenoyl phenylalanine. (B) AFM image of the hydrogel. (C) SEM image of the hydrogel. (D) TEM image of the hydrogel [20]. Copyright © 2013 American Chemical Society. Adapted with permission.

1.4 [2.2]Paracyclophane

[2.2]Paracyclophane has an interesting structure which involves two facing benzene rings that bound in para position with two ethyl groups. Both experimental and theoretical studies have shown that [2.2]paracyclophane exhibits conductivity on a platinum electrode as a single molecule [23]. Similarly, due to the π-π interaction of graphene layers of graphite has conductivity on vertical plane as well as due to its π conjugation on the horizontal plane [24]. However, it is known that the distance between two graphene rings on graphite is 3.35 Å, where, in [2.2]paracyclophane, it is shorter than the optimum π-π stacking. The distance is measured approximately as 3.09 Å on non-bridged and 2.78 Å on bridged carbon-carbon bonds (Figure 8) [25]. The distances alter because the aromatic rings on the core are distorted due to the ring strain. This unique geometry of [2.2]paracyclophane provides an easier electron transfer between two rings and provides the paracyclophanoyl compounds better conductivity.

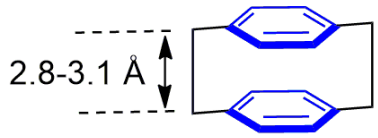

[2.2]Paracyclophane

Figure 8. Molecular structure of [2.2] paracyclophane and the distance between aromatic rings.

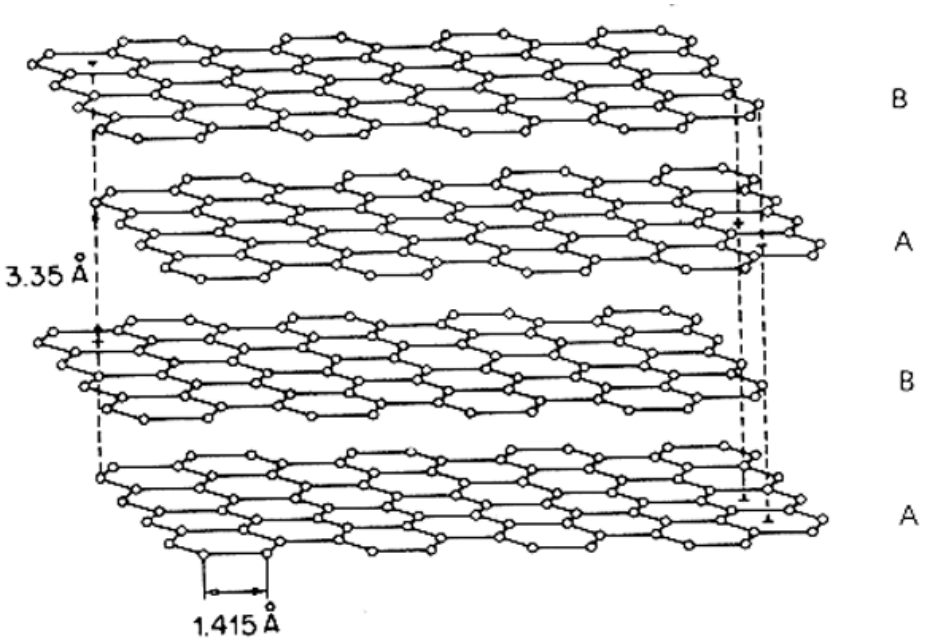

Figure 9. Molecular structure of graphite and the distance between graphene layers.

This extraordinary property of [2.2]paracyclophane has been used for organic electronic applications. As it is shown in Figure 10, Seferos and co-workers [26] obtained a comparable conductivity when paracyclophane and aromatic compound derivatives were bound to gold electrodes with their sulfur atoms. With this study, supporting with theoretical calculations, Seferos has shown that π-π interaction of aromatic rings on paracyclophane is as powerful as π conjugation.

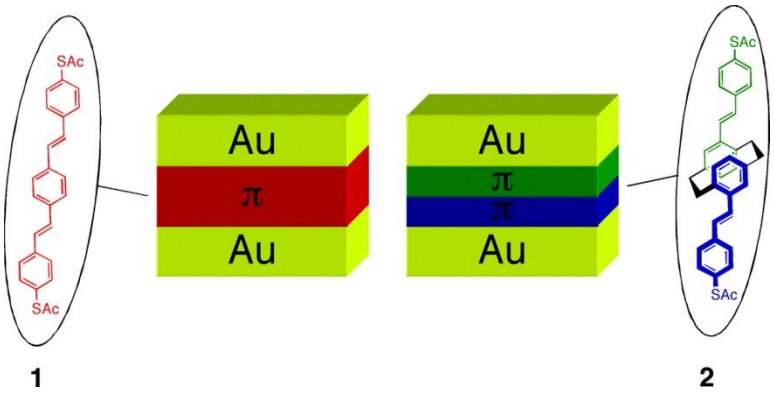

Figure 10. Analysis of conductivities of paracyclophane and styrene derivatives between gold electrodes [23]. Copyright © 2010 American Chemical Society. Adapted with permission.

Similarly, in 2013, Guldi's group [27] added C_{60} molecule to one ring of paracyclophane and added porphyrin ring to the other ring and demonstrated that there was an electron transfer between those rings (Figure 11). Furthermore, they added more than one paracyclophane rings between those groups and provided electron movement.

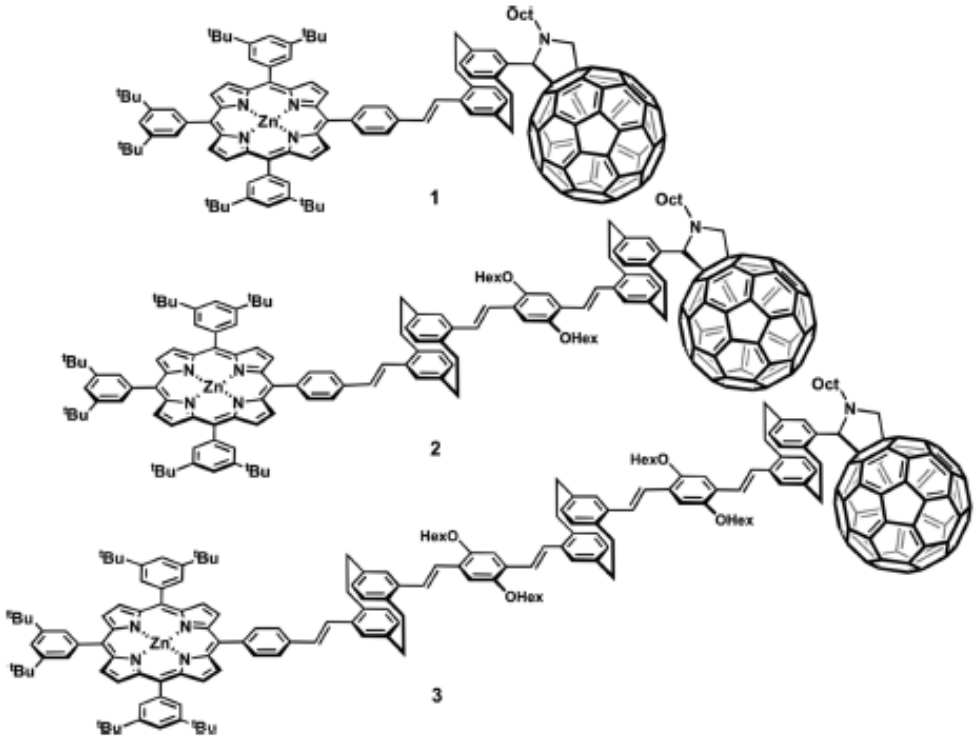

Figure 11. Paracyclophane derivatives synthesized by Guldi [27].

1.5 Organic field-effect transistors (OFETs)

Principally, field-effect transistors (FET) work like capacitors. Between two resistance connections which are the drain and source electrodes, one plate of FETs operates as a conducting channel. The second plate is the gate electrode where the voltage is applied to inflect the density of charge carriers in the channel [28]. Although FET was introduced in 1930 by Lilienfeld [29], first fabrication of silicon-based metal-oxide-semiconductor FET (MOSFET), which is the most conspicuous component of microelectronics, was done in 1960 by Kahng and Atalla [30].

It is known that approximately all organic solids are recognized as insulators. However, electrons can move also in organic crystals providing that the molecule contains π-conjugate system. This movement provides the crystals electrical conductivity [31]. Application of organic electronics in field-effect transistors (OFETs) was classified as possible materials for electronic devices after the study of electrochemically polymerization of thiophene by Koezuka in 1987 [32].

1.5.1 Application of OFETs in conductive peptide hydrogels

The inclusion of π-conjugated conductive organic molecules into biologically relevant compounds suggests great potential to build bioelectronic materials [33, 34]. Studies of OFET devices built by using π-conjugated systems attached to peptide subdivisions are prominent by many researchers. For example, in 2012, Tovar and co-workers [35] used peptide-linked oligothiophene hydrogelators (Figure 12) as active layers of FETs and obtained hole mobilities as 3.8×10^{-5} $cm^2.V^{-1}.s^{-1}$.

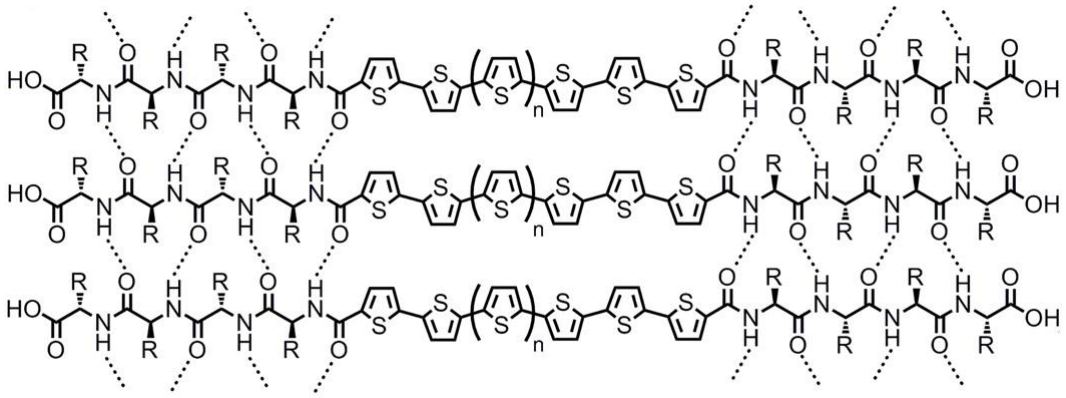

Figure 12. Tovar's peptide-linked oligothiophenes [32]. Copyright © 2012 American Chemical Society. Adapted with permission.

Another study of Holmes and co-workers in 2010 [36], α-helical lysine based sexithiophene was used as semiconductor and obtained field-effect hole mobilities as 1.9×10^{-7} $cm^2.V^{-1}.s^{-1}$.

In the recent study of Tovar and co-workers [37], they bound three or four water soluble oligopeptides to different π-systems (benzotrithiophene, decacyclene triimide and meso-substituted porphyrin) as shown in Figure 13 and investigated their field-effect hole mobilities.

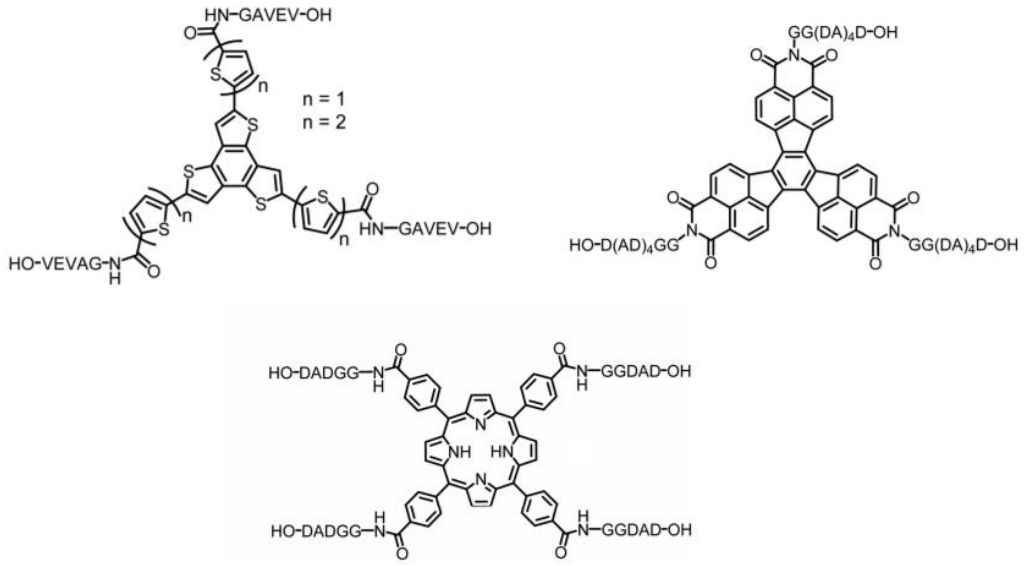

Figure 13. Structures of Tovar's π system attached peptide trimers and tetramer [37].

In the benzotrithiophene-based peptide trimers, they obtained field-effect hole mobilities as 4.6×10^{-5} and 6.6×10^{-5} $cm^2.V^{-1}.s^{-1}$. This demonstrated that increasing thiophene groups increases the mobility values. In the meso-substituted porphyrin-based peptide tetramer system, they obtained field-effect hole mobilities as 7.2×10^{-5} $cm^2.V^{-1}.s^{-1}$. However, in decacyclene triimide-based peptide trimer system, they could not obtain field-effect hole mobilities.

1.6 Aim of the study

Semi-conductive π-conjugated peptide-based hydrogelators using low molecular weight molecules is significant for drug delivery, biocompatitive materials and organic electronic devices. As it has been mentioned, the lowest molecular weight hydrogelator was reported by Zhang and co-workers in 2013 [20]. It can be considered that coupling of [2.2]paracyclophane which has a similar structure with ferrocene, with a single aromatic amino acid might be a semi-conductive hydrogelator because of the π-π interaction of both [2.2]paracyclophane and aromatic amino acid (Scheme 1).

In the light of this, our aim was to synthesize both ferrocenoyl phenylalanine (**FF**) and [2.2]paracyclophanoyl amino acids using phenylalanine (**PC-F**), tyrosine (**PC-Y**) and tryptophan (**PC-W**), make their hydrogels and compare their electrical properties.

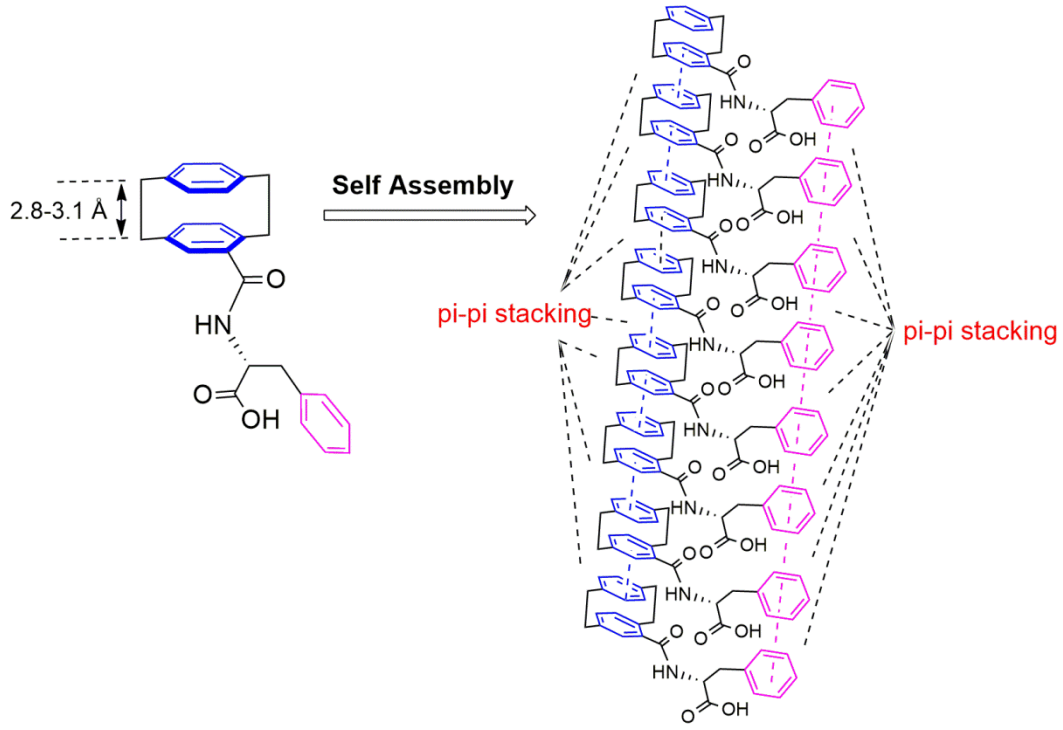

Scheme 1. Predicted self-assembly of [2.2]paracyclophanoyl phenylalanine.

CHAPTER 2

RESULTS AND DISCUSSION

2.1 Synthesis of ferrocenoyl phenylalanine

In this study, the first step was investigation of electrical properties of ferrocenoyl phenylalanine hydrogels and measuring their field-effect hole mobilities. For that reason, starting with commercially available ferrocenecarboxaldehyde, ferrocenecarboxylic acid (**2**) was synthesized following the literature procedure [38]. Potassium permanganate solution in water was used for this synthesis and pure compound **2** was obtained in good yield (74%).

Before the coupling reaction, commercially available L-phenylalanine was converted into its methyl ester **4** using thionyl chloride ($SOCl_2$) and methanol (Scheme 2). After this protection, coupling reaction between compound **2** and compound **4** was applied in basic medium using HOBt and HBTU as coupling agents. Ferrocenoyl phenylalanine methyl ester (**3)** was obtained and purified with column chromatography. Methyl protection on carboxylic acid was removed using basic hydrolysis to obtain crude compound **5** which was purified by column chromatography to get an overall yield of 32% starting from ferrocenecarboxaldehyde. ^{1}H NMR data of compound **5** was in consistent with literature (Figure 14) [20]. Overall synthesis of compound **5** is shown in Scheme 3.

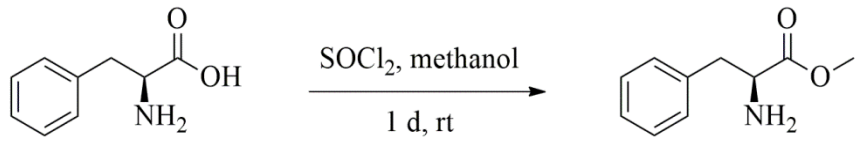

Scheme 2. Synthesis of L-phenylalanine methyl ester.

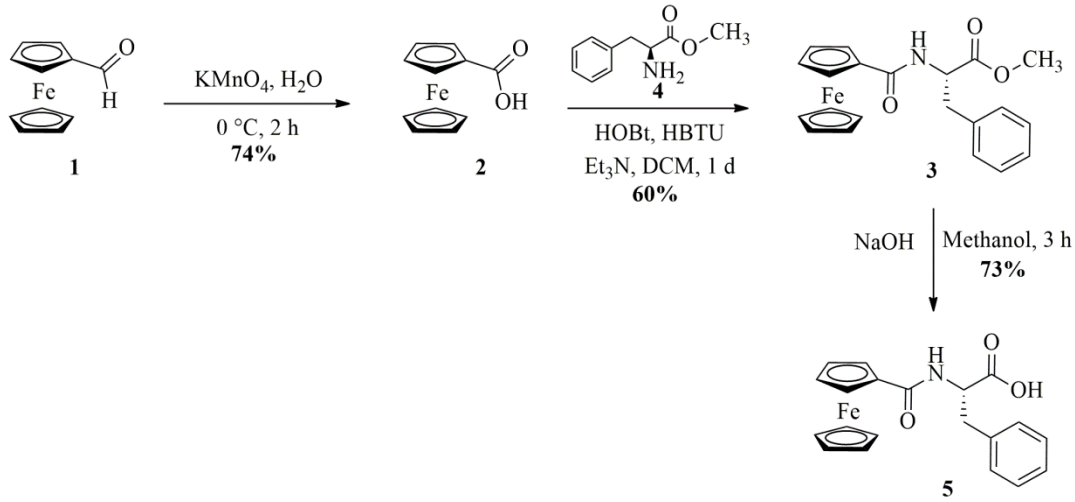

Scheme 3. Overall synthesis of ferrocenoyl phenylalanine **(FF)**.

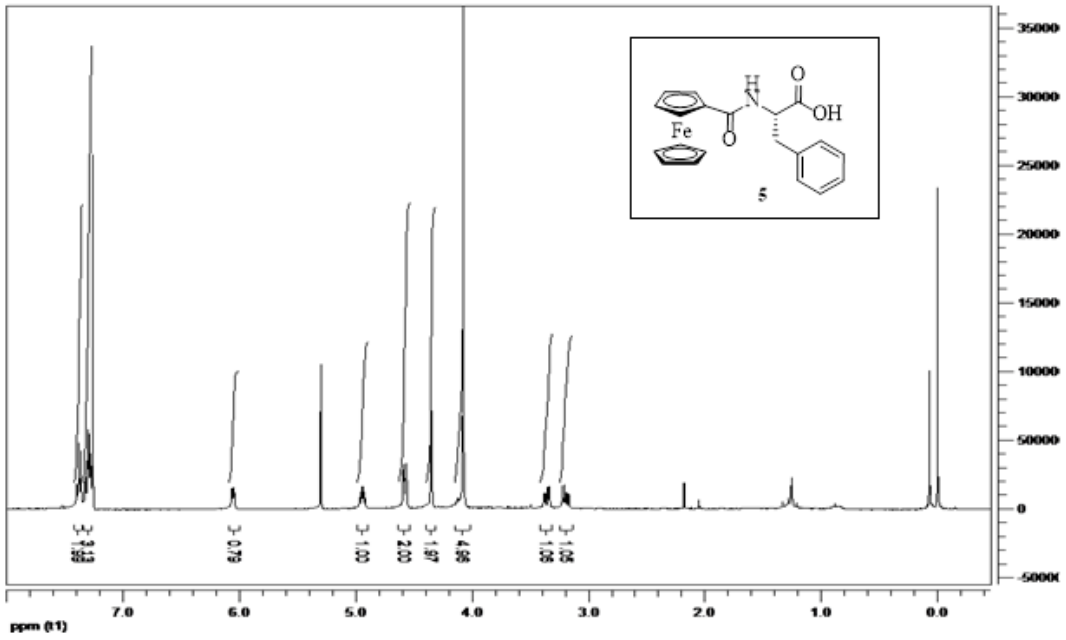

Figure 14. ^{1}H NMR spectrum of ferrocenoyl phenylalanine (**FF**).

After synthesizing compound **5**, it was dissolved in acetonitrile and water mixture, freeze dried to obtain solid ferrocenoyl phenylalanine (**FF**). On the other hand, 10

mM of phosphate buffer solution was prepared using sodium phosphate dibasic (NaH_2PO_4) and sodium phosphate monobasic (Na_2HPO_4). Then the pH of solution was adjusted to 7.4. Solid **FF** was then dissolved in 50 μL of DMSO. To this solution 1 mL of prepared buffer solution was added and observed partial precipitation. After the mixture was sonicated using an ultrasonic bath for 5 to 7 minutes, **FF** hydrogel was obtained. This procedure was repeated three more times and four **FF** hydrogels were obtained (Figure 15).

Figure 15. FF hydrogels.

2.1.1 Electrical properties of FF hydrogels

After **FF** hydrogels were obtained, the electrical properties of these hydrogels were analyzed by Çiğdem Çakırlar from Sait Eren San's research group in Gebze Technical University. HP-4194A Gain/Phase impedance analyzer was used for this analysis. 0.75 mm thick films prepared using both materials were compressed between two parallel plates with dropping method and electrical analysis was performed.

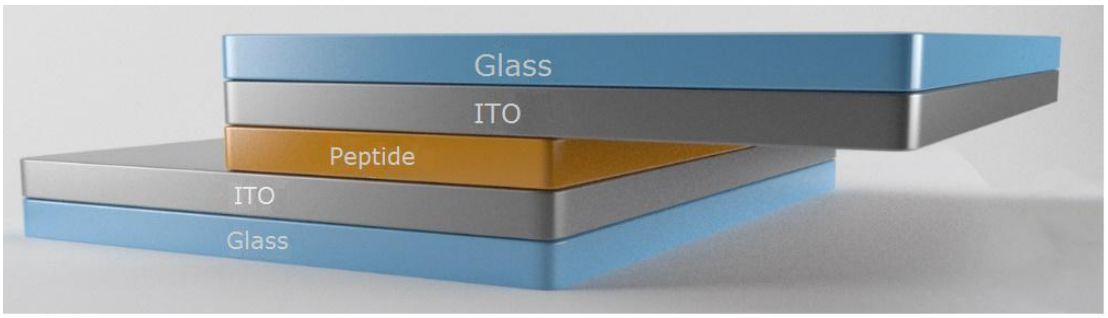

Figure 16. Schematic diagram of the samples prepared for dielectric analysis.

Measurements were done at room temperature (25℃) using alternating current (AC) between 100 Hz and 15 MHz. AC conductivity mechanisms (σ) and frequency dependent real dielectric constants (ε') of the samples were investigated.

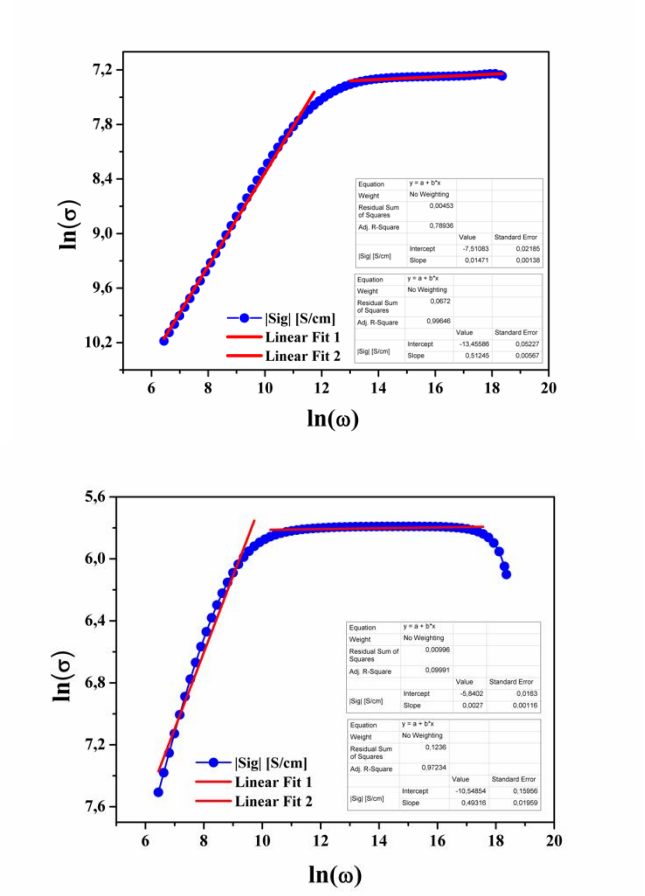

Figure 17. ln(σ)- ln(ω) graphics of (a) **FF** hydrogels and (b) dried overnight hydrogels.

Conductivity of **FF** hydrogels and dried overnight hydrogels were measured approximately as 10^{-3} $\Omega^{-1}cm^{-1}$ and 10^{-4} $\Omega^{-1}cm^{-1}$ respectively. This result indicated that the reason of conductivity is self-assembly of **FF**. It is shown that the conductivity value due to salts in dried hydrogel was very low comparing with the conductivity of **FF**.

AC conductivity mechanisms were investigated using Jonscher's universal conductivity law ($\sigma = \sigma_0 + A\omega^s$). σ_0 was determined as DC conductivity component and $A\omega^s$ was determined as AC conductivity component. ln(σ)- ln(ω) curves were fitted using equation of a straight line ($y = ax + b$). The slopes of these fits were calculated and obtained "s" parameter of the universal conductivity law. This "s" parameter indicated the variations of the frequency dependent conductivity mechanism. These variations are shown in Table 2. The conductivity mechanisms of two samples were the same in low and high frequency range. Correlated Barrier Hopping (CBH) conductivity mechanism was observed in low frequency range and DC conductivity mechanism was observed in high frequency range.

Table 2. s parameters and frequency dependent conductivity mechanism

s-parameter	**Conductivity mechanism**
s≈0	DC conductivity
0<s<0.7	Correlated Barrier Hopping (CBH)

The variation of frequency dependent dielectric constant (ε') is shown in Figure 13. In low frequency range, the effect of water molecules in **FF** hydrogels to the polarization and the sudden change depending on this result is clearly visible. However, there is a more stable case in the dried **FF** hydrogels due to the absence of water molecules.

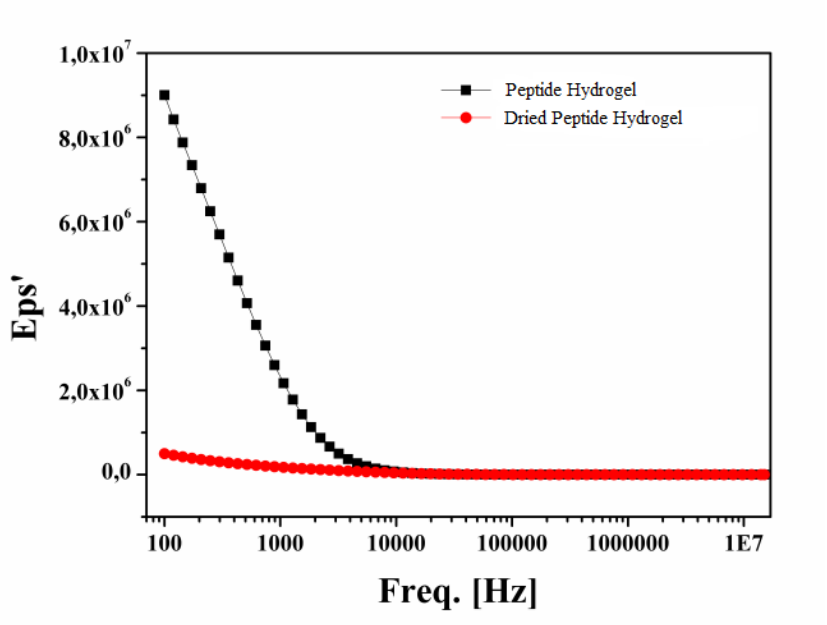

Figure 18. Change in frequency dependent dielectric constants of **FF** hydrogels and dried hydrogels.

I-V measurements of **FF** hydrogels were done using gold electrodes having 100 μm channel band. The measurement was performed between 0 to 60 V using 0.109 s steps. Mobility (μ) was calculated using Charge Carrier Extraction by Linearly Increasing Voltage (CELIV) method. The formula indicated below was used for these calculations. In that formula, V is the applied voltage per unit time, d is the channel band, ΔJ is current density difference on non-lineer zone and J_0 is the maximum current value in lineer zone.

$$\mu = \frac{2d^2}{3\frac{V}{t}t_{max}^2(1 + 0.36\frac{\Delta J}{J_0})}$$

Using this equation, mobility (μ) was calculated as 2.4 x 10^{-5} cm^2/Vs.

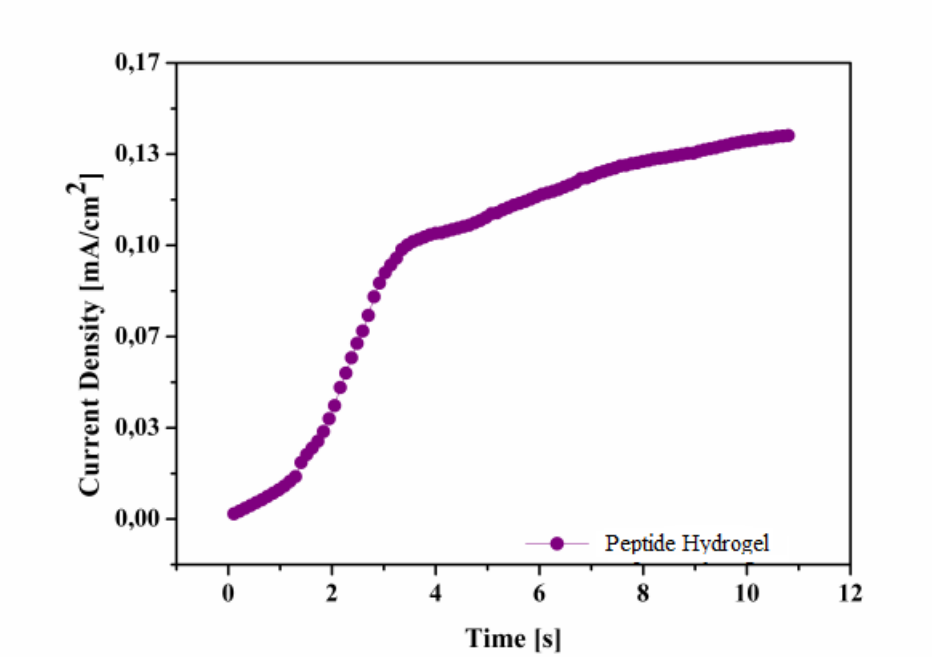

Figure 19. Current voltage slope of FF hydrogels.

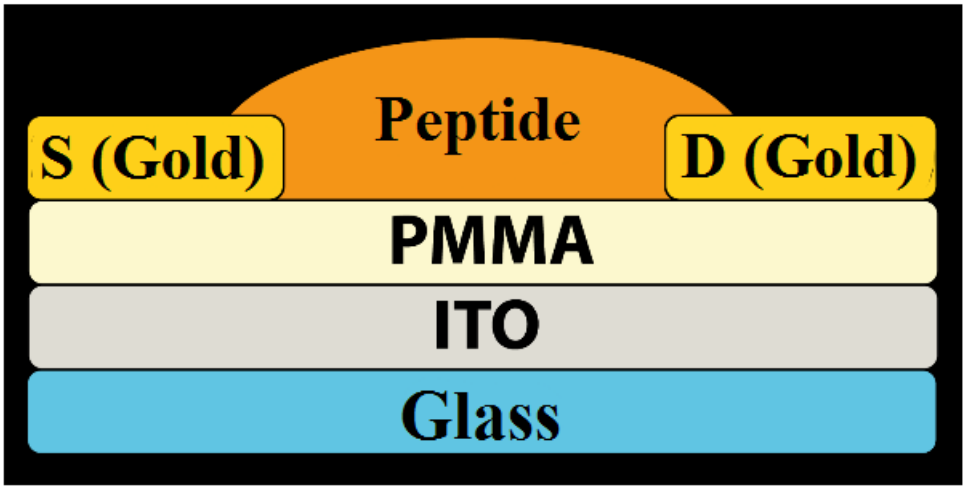

Figure 20. Schematic diagram of produced OFETs.

Ferrocenoyl phenylalanine hydrogel-based Organic Field Effect Transistor (OFET) work was done using a bottom gate-top contact electrode design. Indium Tin Oxide (ITO) coated glass was chosen as the gate electrode. Poly (methyl methacrylate) (PMMA) was selected as gate insulator. PMAA was coated on the previous cleaned ITO coated glass by spin coating method. Gold source and drain electrodes were coated by using thermal evaporator. **FF** hydrogels, as the

semiconductor layer, coated to the channel between the S-D electrode using dropping method.

I-V analysis of generated OFETs was done at room temperature using Keitley 4200 SCS. As it is known, the reduction of the operating voltage of OFETs has a great importance according to the integration into low power electronic applications. OFETs working at low voltages (less than 1 V), prepared using **FF** hydrogel as semi-conductor, were produced (Figure 21). With this study, solution processed OFET production was achieved for electronic applications requiring low voltage and low power.

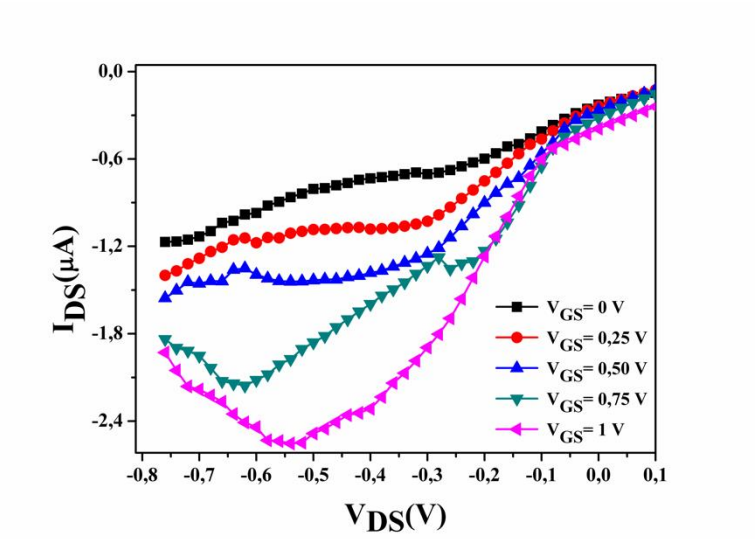

Figure 21. Output graphics of produced OFETs.

2.2 Synthesis of [2.2]paracyclophane-2-carboxylic acid

After investigation of electrical properties of ferrocenoyl phenylalanine (FF), the second part of the study was to synthesize [2.2]paracyclophanoyl phenylalanine, make its hydrogel and compare its electrical properties with **FF** hydrogels. To make the coupling reaction of [2.2]paracyclophane and phenylalanine, carboxylic acid derivatives of paracyclophane was needed. Therefore, based on the literature [39], [2.2]paracyclophane-2-carboxylic acid was synthesized starting from commercially available [2.2]paracyclophane (Scheme 4).

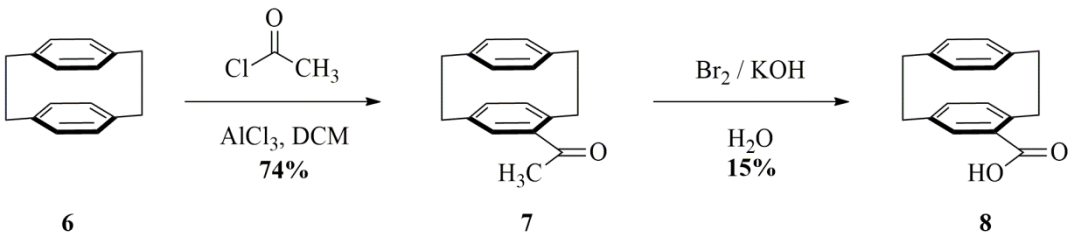

Scheme 4. Synthesis of [2.2]paracyclophane-2-carboxylic acid.

The first step of the synthesis was Friedel-Craft reaction with acetyl chloride in DCM to get 2-acetyl-[2.2]paracyclophane in good yield (74%). In the second step, acetyl group was converted into carboxylic acid by using haloform reaction with Br_2/NaOH in water to give [2.2]paracyclophane-2-carboxylic acid with a yield of 80%. However, when the scale of the second reaction was increased to 1 mmol, haloform reaction could not be achieved. Therefore, an alternative route was applied (Scheme 5). In this synthetic route, compound **6** was formylated to get [2.2]paracyclophane carboxaldehyde (**9**) using Rieche formylation [40]. Then, compound **9** was oxidized to [2.2]paracyclophane-2-carboxylic acid using hydrogen peroxide and sodium hydroxide at high temperature [41]. However, low yield (30%) was observed in this step. Hence, oxidation of compound **9** was done using potassium permanganate [38] and high yield (90%) was obtained (Scheme 6).

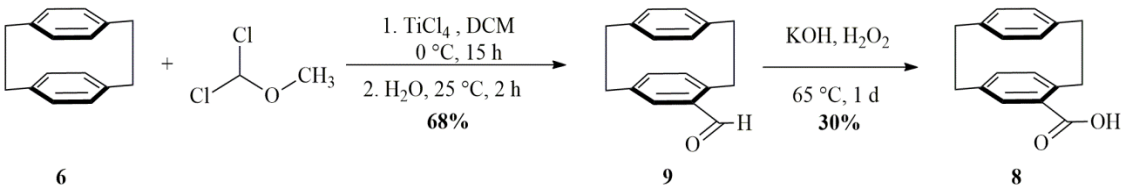

Scheme 5. Synthesis of [2.2] paracyclophane-2-carboxylic acid (**8**) from aldehyde derivative **9**.

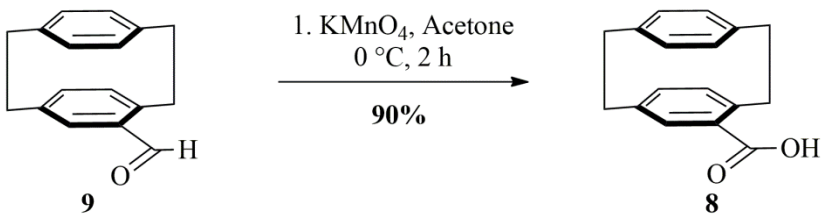

Scheme 6. Synthesis of [2.2]paracyclophane-2-carboxylic acid (**8**) with $KMnO_4$.

2.3 Synthesis of [2.2]paracyclophane mono amino acid (PC-AA) derivatives

After synthesizing and purification of compound **8**, [2.2]paracyclophanoyl mono amino acid derivative was synthesized using the same method that was used for the synthesis of ferrocenoyl phenylalanine [20] (Scheme 7).

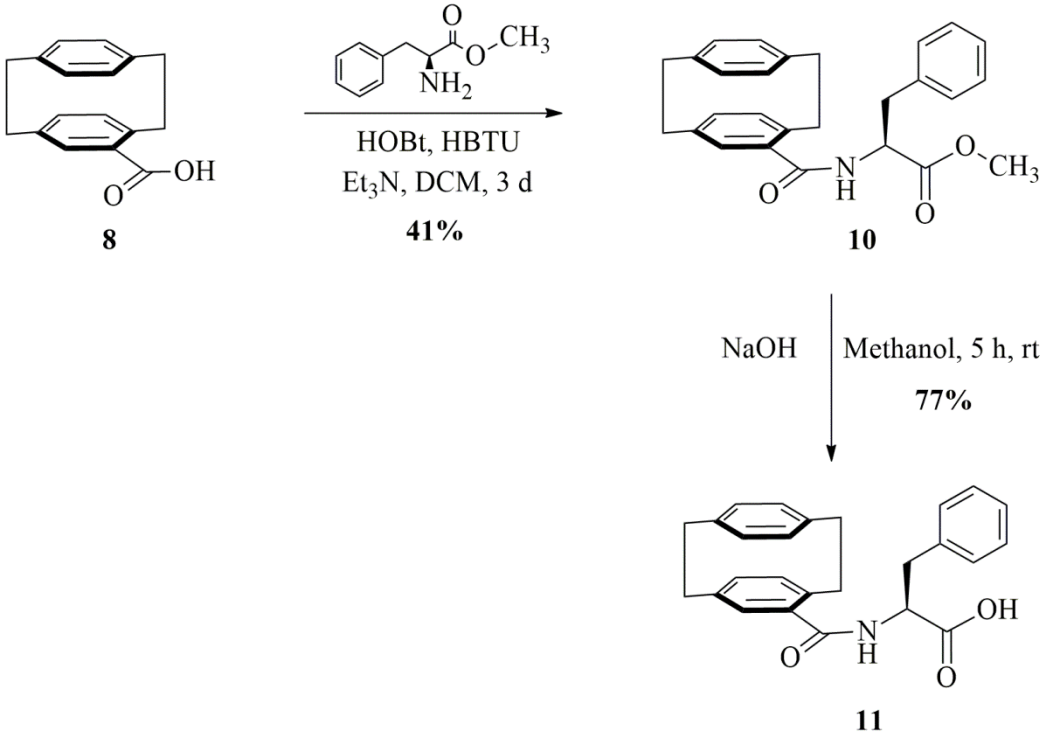

Scheme 7. Synthesis of [2.2]paracyclophanoyl phenylalanine.

[2.2]paracyclophane-2-carboxylic acid was coupled with phenylalanine methyl ester in the presence of HBTU and HOBt as coupling agents. However, low yield was obtained (overall yield is 31%) and purifying the compound **11** using flash

column chromatography was troublesome because of the low Rf value even in highly polar eluents (DCM, ethyl acetate and methanol). Therefore, other mono (Scheme 8) and dipeptide derivatives were synthesized using solid phase peptide synthesis (SPPS) method (Scheme 9).

For solid phase peptide synthesis, 2-chlorotrytil chloride resin was chosen to get the C-terminal of peptide derivatives as carboxylic acids. The coupling of first amino acid on the resin was obtained by mixing Fmoc protected amino acid and resin in basic medium. Then, the mixture was washed with DMF and treated with DCM/Methanol/DIEA (80:15:5) solution in order to cap the unreacted sites on resin. The mixture was washed with DMF again and treated with 20% piperidine solution in DMF to remove Fmoc protecting group. Then the resin was reacted with second amino acid which was activated by HBTU and DIEA using standard solid phase peptide synthesis method. After this coupling reaction, Fmoc protection group was removed using 20% piperidine solution in DMF. As a final step, [2.2] paracyclophane-2-carboxylic acid was activated by HBTU and DIEA and reacted with resin using the same method. To remove the side chain protecting groups on amino acids and cleave the peptide derivatives from resin, a cleavage cocktail was prepared. This cleavage cocktail containing 95% trifluoroacetic acid (TFA), 2.5% water and 2.5% triisopropylsilane (TIPS) was reacted with resin for 1 hour and the solution was collected by filtration. TFA and other residues in solution were removed under vacuum and the peptide derivative was triturated with cold diethyl ether. The precipitate was then dissolved in acetonitrile and water, and freeze dried to get fine solids.

For the synthesis of PC-AA derivatives, 0.1 mmol of 2-chlorotrytil chloride resin was used and 5.5 eq. (0.55 mmol) of first amino acid and 3.0 eq. (0.30 mmol) of [2.2]paracyclophane-2-carboxylic acid were added.

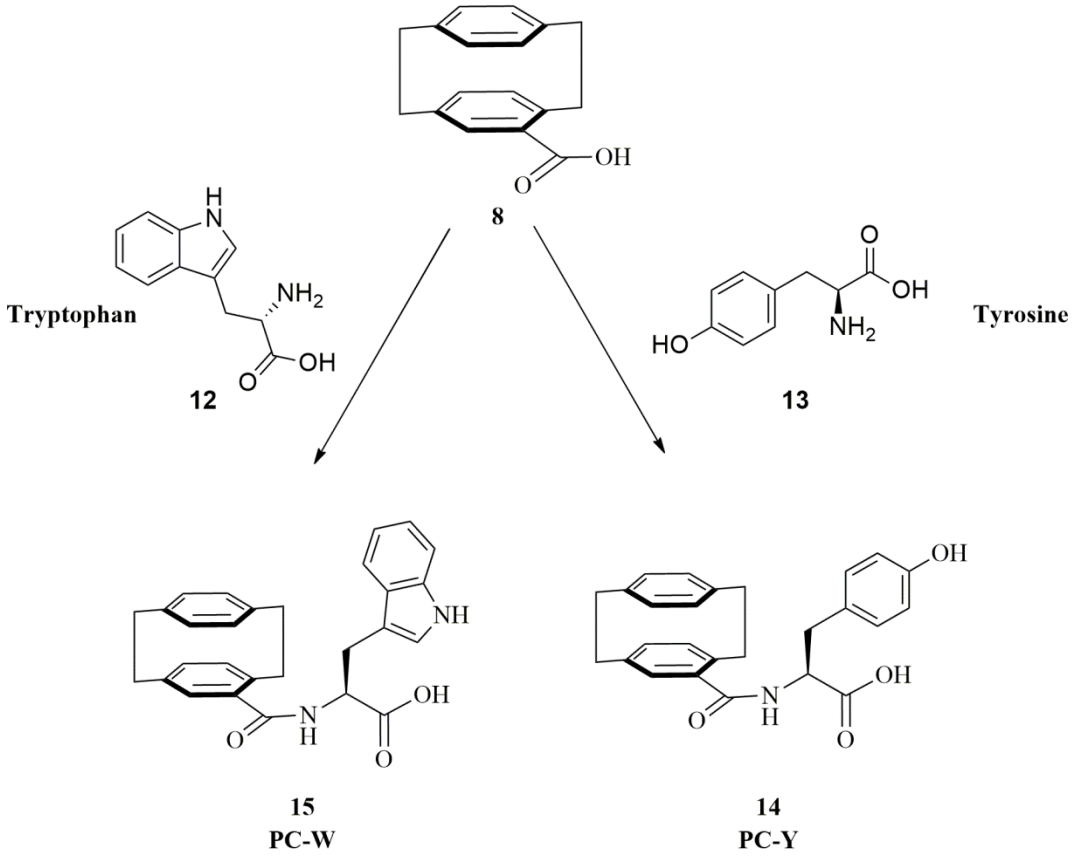

Scheme 8. Synthesis of **PC-W** and **PC-Y**.

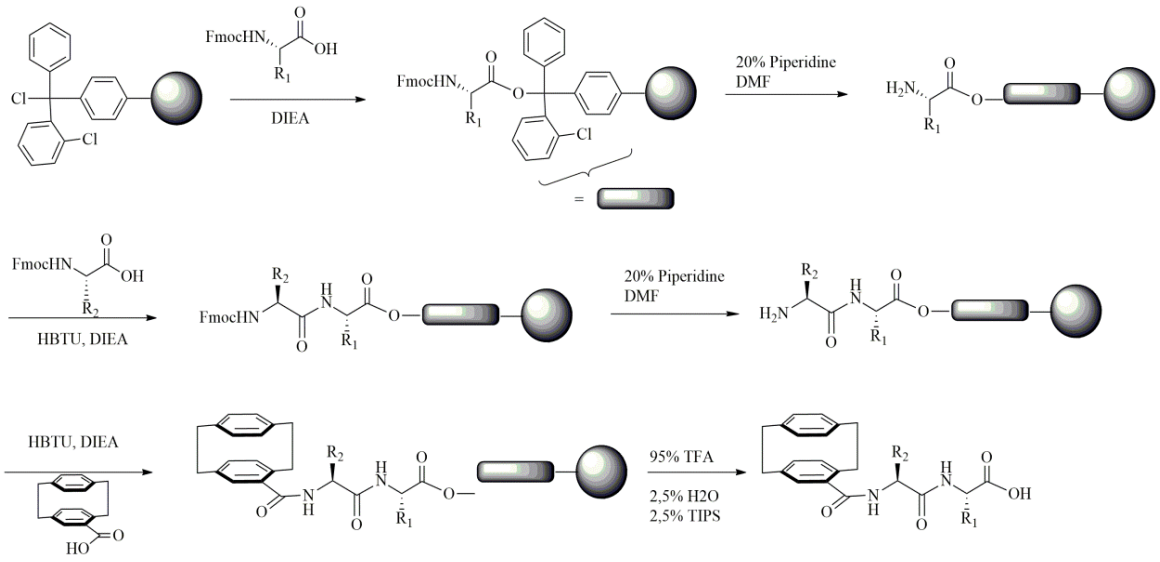

Scheme 9. Solid Phase Peptide Synthesis of PC-dipeptide derivatives.

The characterization of [2.2]paracyclophanoyl phenylalanine (**PC-F**), [2.2]paracyclophanoyl tyrosine (**PC-Y**) and [2.2]paracyclophanoyl tryptophan

(**PC-W**) were performed by HPLC, HRMS, ^{1}H NMR and ^{13}C NMR spectroscopies.

2.4 Synthesis of [2.2]paracyclophanoyl dipeptide derivatives

In order to increase the water solubility of paracyclophane derivatives, a second amino acid with high hydrophilicity (aspartic acid, glutamic acid and arginine) was introduced into the structure for each PC-AA. As a result of this, new nine [2.2]paracyclophanoyl dipeptides (Figure 23) were synthesized using SPPS starting from 2-chlorotrytil chloride resin. These peptides were analyzed by HPLC and HRMS.

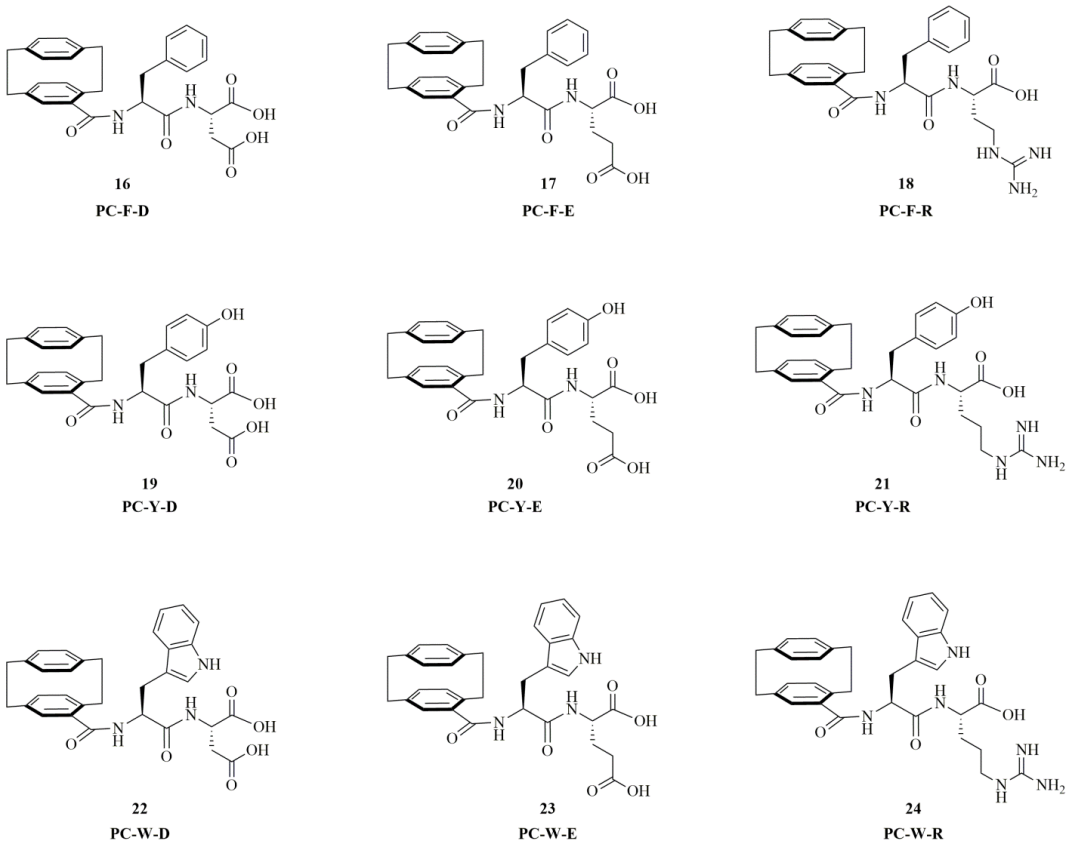

Figure 22. Structures of paracyclophane dipeptides.

2.5 Hydrogelation of [2.2]paracyclophane derivatives

First of all, hydrogelation of **PC-F** was tried using the same method as applied for **FF**. However, as the first drop of buffer solution was added to solution of **PC-F** in DMSO, complete precipitation was observed as it is shown in Figure 24.

Figure 24. Precipitation of [2.2] paracyclophanoyl phenylalanine.

Then, the other mono amino acid derivatives (**PC-Y** and **PC-W**) were tested to form hydrogels but again precipitations were observed. Different parameters, such as concentration, temperature and time of sonication, were changed as shown in Table 3. Yet, hydrogelation could not be observed in any derivatives. Even though all PC-AAs were dissolved at high temperature (80 °C) and sonicated at room temperature or at 50 °C, precipitations were observed after they cooled down to room temperature.

Table 3. Hydrogelation attempts of [2.2]paracyclophane mono amino acids with different parameters.

Concentration (mg/mL)	Organic Solvent	Temperature of mixture	Time of Sonication	Temperature of Sonic Bath
5 mg/mL	DMSO	25 ℃	5 min	25 ℃
5 mg/mL	DMSO	25 ℃	15 min	25 ℃
5 mg/mL	1-4 Dioxane	25 ℃	10 min	25 ℃
3 mg/mL	DMSO	25 ℃	15 min	25 ℃
3 mg/mL	DMSO	80 ℃	15 min	25 ℃
3 mg/mL	DMSO	80 ℃	30 min	25 ℃
3 mg/mL	DMSO	80 ℃	10 min	50 ℃

Hydrogelation of nine PC dipeptide derivatives with different parameters has also been tried as shown in Table 4. Yet, no hydrogel was observed in any derivatives.

Table 4. Hydrogelation attempts of paracyclophane dipeptides with different parameters

Concentration (mg/mL)	Organic Solvent	Temperature of mixture	Time of Sonication	Temperature of Sonic Bath
5 mg/mL	DMSO	25 ℃	5 min	25 ℃
5 mg/mL	DMSO	25 ℃	15 min	25 ℃
5 mg/mL	DMSO	25 ℃	30 min	25 ℃
8 mg/mL	DMSO	25 ℃	15 min	25 ℃
8 mg/mL	DMSO	25 ℃	5 min	25 ℃
3 mg/mL	DMSO	25 ℃	15 min	25 ℃
8 mg/mL	DMSO	50 ℃	10 min	25 ℃
8 mg/mL	DMSO	50 ℃	10 min	50 ℃

2.6 Resolution of [2.2]paracyclophane-2-carboxylic acid

It is known that mono substituted paracyclophanoyl molecules are chiral molecules while mono substituted ferrocenoyl molecules show no chirality. Twelve paracyclophane derivatives were synthesized starting with racemic [2.2] paracyclophanoyl-2-carboxylic acid. And it should be noted that Zhang and co-workers observed partially hydrogelation when racemic **FF** was used. It was considered that diastereomic mixture may disrupt self-assembly and prevent hydrogelation. Therefore, **PC-F** was synthesized starting from enantiopure [2.2]paracyclophane-2-carboxylic acid (**8**) which was obtained by the chiral resolution of its racemic form using the procedure in the literature [39] as shown in Scheme 9.

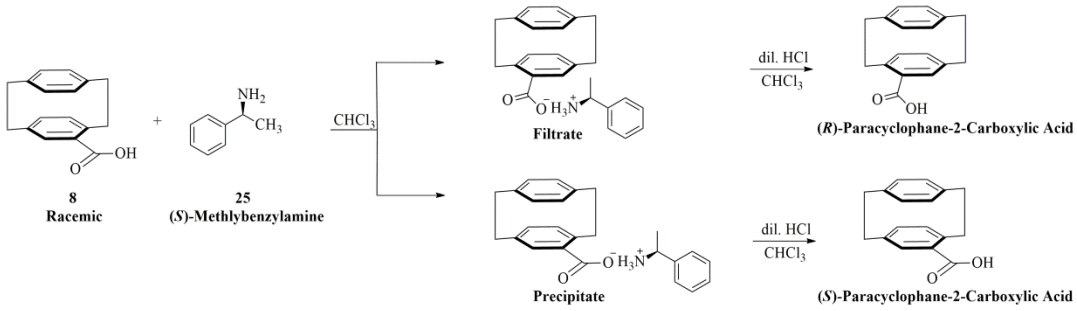

Scheme 10. Resolution of [2.2] paracyclophane-2-carboxylic acid.

For resolution of compound **8** into its enantiomers, (*S*)-(-)-α-methylbenzylamine was used to get diastereomeric salt mixture. Salt formation reaction was monitored by TLC and after completion, cold ether was added to get rid of the unreacted organic residues. Ether was then evaporated under reduced pressure and one diastereomer of salt was precipitated with cold ethanol. Filtrate and precipitate was separated and turned to free carboxylic acids with dilute HCl.

Optical rotation of (*S*)-(+)-[2.2]paracyclophane-2-carboxylic acid was found as $[\alpha]_D = +162^o$ (c = 1.0 x 10^{-2} g/mL, $CHCl_3$) where literature value is $[\alpha]_D = +162^o$.

Optical rotation of (*R*)-(-)-[2.2] paracyclophane-2-carboxylic acid was found as $[\alpha]_D = -153^o$ (c = 1.0 x 10^{-2} g/mL, $CHCl_3$) where literature value is $[\alpha]_D = -157^o$.

Hyrogelation of enantiopure **PC-F** could not be completed yet.

2.6 Conclusion

In conclusion, ferrocenoyl phenylalanine was synthesized and its hydrogels were obtained successfully. The electrical properties of these hydrogels were studied and obtained comparable conductivity (10^{-3} $\Omega^{-1}cm^{-1}$ for **FF** hydrogels and 10^{-4} $\Omega^{-1}cm^{-1}$ for dried **FF** hydrogels) with the peptide hydrogels in the literature. Hole mobility measurement was also performed (2.4 x 10^{-5} cm^2/Vs) and **FF** hydrogel-based OFETs which require low voltage and power were developed.

For the second part of the study, three [2.2]paracyclophanoyl mono amino acid derivatives and nine [2.2]paracyclophanoyl dipeptide derivative were synthesized successfully to form their hydrogels. However, it was failed despite using different parameters individually. [2.2]paracyclophanoyl phenylalanine was synthesized again using single enantiomer of [2.2] paracyclophane-2-carboxylic acid but hydrogelation studies could not be completed.

CHAPTER 3

EXPERIMENTAL

3.1 Materials and methods

[2.2] paracyclophane and ferrocenecarboxaldehyde were supplied from Sigma Aldrich, Germany.

Fmoc-Amino acids were supplied from Chem-Impex Inc, USA.

HPLC grade solvents were supplied from Sigma Aldrich, Germany.

Other solvents are technical grade. They were purified, when necessary, using distillation method.

All reactions except the compounds synthesized using SPPS method were examined by TLC on silica gel plates and visualized by UV-light at 254 nm wavelength. Chromatographic separations were carried out by glass precoated silica gel with particle size of 0.063-0.200 mm.

Nuclear magnetic spectra were read in $CDCl_3$ and CD_3OD on Bruker Spectrospin Advance DPX 400 spectrometer. Chemical shifts were received in parts per million (ppm) with TMS as internal reference. NMR spectra of the compounds are given in Appendix A.

HPLC chromatograms were read on an Agilent 1100 Series. HPLC chromatograms of compounds are given in Appendix B.

For lyophilization, freeze dryer, Telstar Cryodos instrument was used.

For sonication, KUDOS HP Series 53kHz high frequency ultrasonic cleaner was used.

3.2 Synthesis of ferrocene carboxylic acid

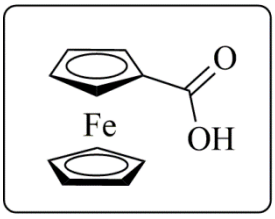

Based on the literature [38], 0.750 g (3.50 mmol) of ferrocene carboxaldehyde was dissolved in acetone (35 mL) at 0 °C. 1.9 g (12 mmol) of $KMnO_4$ in water (7 mL) was added to this solution and stirred for 2 hours. After 2 hours, 1 M NaOH solution (4 mL) was added and the mixture was stirred for 15 minutes at room temperature. Additional 1 M of NaOH solution (2 mL) was added. The dark colored reaction mixture was filtrated and orange liquid was obtained. The filtrate was extracted three times with diethyl ether to remove ferrocene carboxaldehyde. 1 M HCl was added to the solution until the pH was 4 and extracted five times with diethyl ether. Organic phase was then dried with $MgSO_4$, filtrated and the solvent was removed under low pressure using rotary evaporator and obtained reddish orange solid. The solid was then purified by flash column chromatography (EtOAc:Hexane = 3:1, Rf = 0.2) on silica gel and obtained 600 mg (2.61 mmol) of orange solid. Yield is 74%.

^{1}H NMR ($CDCl_3$, 400 MHz): δ (ppm) 4.19 (s, 5H), 4.40 (t, *J* = 2.0 Hz, 2H), 4.80 (t, *J* = 1.6 Hz, 2H).

3.3 Synthesis of L-phenylalanine methyl ester

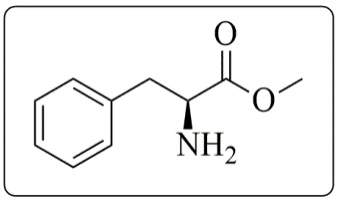

570 mg (3.45 mmol) of L-phenylalanine was dissolved in methanol (10 mL). To this solution, 0.40 mL (5.5 mmol) of $SOCl_2$ was added dropwise at 0 °C and allowed to warm to room temperature. The reaction mixture was then stirred for overnight at room temperature and the solvent was removed under reduced pressure. 550 mg (3.07 mmol) of pure L-phenylalanine methyl ester was obtained. Yield is 89%.

^{1}H NMR (CD_3OD, 400 MHz): δ (ppm) 3.14 (s, 2H), 3.74 (s, 3H), 4.10-4.14 (m, 1H), 7.17-7.28 (m, 5H).

3.4 Synthesis of ferrocenoyl phenylalanine methyl ester

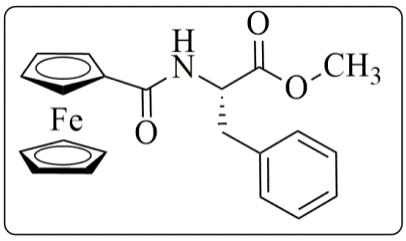

Based on the literature [20], 115 mg (0.500 mmol) of ferrocene carboxylic acid, 210 mg (0.550 mmol) of HBTU and 76 mg (0.55 mmol) of anhydrous HOBt were dissolved in DCM (100 mL) at 0 °C. 190 mL (1.30 mmol) of triethylamine (Et_3N) was added for 1 hour to the stirred reaction mixture for activating the carbonyl group. After 1 hour, 1 equivalent (90 mg, 0.50 mmol) phenylalanine methyl ester salt was added and the reaction was stirred overnight. The reaction mixture was then washed with Na_2CO_3 solution, dilute HCl and extracted with DCM. Organic phase was then dried with anhydrous sodium sulfate, filtrated and the solvent was evaporated under reduced pressure using rotary evaporator and obtained as an orange solid. The solid was then purified by flash column chromatography (DCM:EtOAc:Hexane = 3:1:5) on silica gel and obtained 120 mg (0.307 mmol) of orange oil solid. Yield is 60%.

^{1}H NMR ($CDCl_3$, 400 MHz): δ (ppm) 3.15 (d, *J* = 7.1 Hz, 2H,), 3.85 (s, 3H), 4.06 (s, 5H), 4.25 (s, 2H), 4.48 (d, *J* = 7.1 Hz, 2H), 4.95 (s, 1H), 6.05 (s, 1H), 7.28 (m, 3H), 7.33 (d, *J* = 6.0 Hz, 2H).

3.5 Synthesis of ferrocenoyl phenylalanine

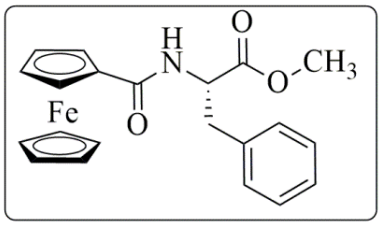

Based on literature [20], 60 mg (0.15 mmol) of ferrocenoyl phenylalanine methyl ester was dissolved in methanol (45 mL) to obtain a 3 mM solution. To this solution, 1 M NaOH solution (20 mL) was added and stirred for 2 hours. After ferrocenoyl phenylalanine methyl ester spot on TLC (EtOAc:Hexane = 1:2) was disappeared, 1 M HCl solution was added until the pH of the mixture was 7 and the solution was evaporated by rotary evaporator to remove leftover methanol. The aqueous orange mixture was then acidified with 1 M HCl. The acidic solution was extracted with DCM four times. Organic phase was then dried over anhydrous Na_2SO_4, filtrated and the solvent was evaporated using rotary evaporator and obtained an orange solid. This solid was dissolved in 4 mL of CH_3CN and 4 mL of deionized water and freeze dried overnight. 45 mg (0.11 mmol) of orange solid was obtained. Yield is 73%.

^{1}H NMR ($CDCl_3$, 400 MHz): δ (ppm) 3.24 (d, *J* = 7.0 Hz, 2H), 4.06 (s, 5H), 4.31 (s, 2H), 4.60 (d, *J* = 7.2 Hz, 2H), 4.95 (s, 1H), 6.22 (s, 1H), 7.28 (m, 3H), 7.33 (d, *J* = 6.0 Hz, 2H).

3.6 Hydrogelation of ferrocenoyl phenylalanine

5 mg of ferrrocenoyl phenylalanine was dissolved in 50 μL DMSO and 1 mL of phosphate buffer solution (pH=7.4, 10 mM) was added to this solution. Sonicated in ultrasonic bath for 7 minutes and hydrogelation was achieved.

3.7 Preparation of FF-hydrogel-based OFET

A solution was prepared using 60 mg PMMA and 1 ml ethyl acetate. This solution was stirred for 6 hours at 70 °C temperature with magnetic stirrer and coated on the previously cleaned ITO coated glasses by spinning with a spin coater for 45 seconds at 1500 rpm. Constructed films were annealed for 15 minutes at 110 °C. Using Veeco Dektak 8 profilometer, film thicknesses were determined as 600 nm. Gold Source (S) –Drain (D) electrodes were coated with a thickness of 100 nm using a Leybold thermal evaporator. **FF** hydrogels, as the semiconductor layer, coated to the channel between the S-D electrode using dropping method.

3.8 Synthesis 2-acetyl [2.2] paracyclophane

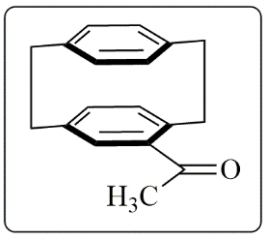

Based on literature [39], 0.860 g (6.45 mmol) of anhydrous aluminum chloride was dissolved in DCM (20 mL). 0.50 mL (7.0 mmol) of acetyl chloride was added to this solution at -30 °C. 750 mg (3.60 mmol) of [2.2]paracyclophane was added and the reaction mixture turns to red with white precipitates. Reaction mixture was stirred for 90 minutes at -30 °C and allowed to warm to room temperature. 1 M of HCl was added (5mL) until the white precipitate was dissolved and the color of the mixture turned to yellowish green. It was stirred overnight at room temperature. Na_2CO_3 solution was added until the pH was 10 and extracted three times with DCM. Organic phase was then dried with $MgSO_4$, filtrated and the solvent was evaporated using rotary evaporator and obtained yellowish solid. The solid was then purified by flash column chromatography (EtOAc:Hexane = 1:4, Rf = 0.8) on silica gel to obtain 660 mg (2.64 mmol) of white solid. Yield is 74%.

^{1}H NMR ($CDCl_3$, 400 MHz): δ (ppm) 2.73 (dt, *J* = 7.8, 4.1 Hz, 1H), 2.88-2.95 (m, 2H), 2.97 (3H, s), 3.09-3.21 (m, 4H), 3.86-3.92 (m, 1H), 6.30 (dd, *J* = 8.0, 4.1 Hz, 1H), 6.41-6.53 (m, 4H), 6.56 (dd, *J* = 8.1, 1.9 Hz, 1H), 6.86 (d, 2.0 Hz, 1H).

3.9 Synthesis [2.2]paracyclophane-2-carboxylic acid from 2-acetyl-[2.2]paracyclophane

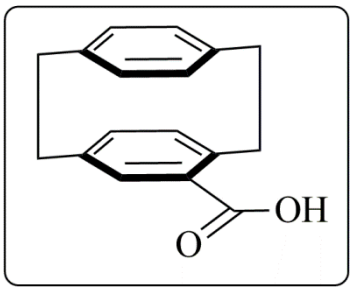

Based on literature [39], 0.56 g (10 mmol) of KOH was dissolved in distilled water (3.0 mL) and 0.22 mL (4.3 mmol) of bromine was added at 0 °C. To the hypobromide solution, 0.33 g (1.3 mmol) of 4-acetyl [2.2]paracyclophane in 4.8 ml of 1,4-dioxane was added slowly and obtained an orange mixture with precipitate. After 2 hours with stirring, ice bath was removed and allowed the mixture to warm to room temperature. Homogenous mixture was obtained and stirred overnight. 8% $NaHSO_3$ solution (15 mL) was added until the pH of the mixture was 7 to remove the excess bromine. Na_2CO_3 solution (2 mL) was added and extracted with DCM three times. Aqueous phase was collected and acidified with 1 M HCl. Mixture was extracted with DCM eight times. Organic phase was then dried over anhydrous $CaSO_4$, filtrated and the solvent was evaporated using rotary evaporator and obtained 260 mg (1.03 mmol) of white solid. Yield is 80%. Rf = 0.45 (EtOAc:Hexane = 1:4)

^{1}H NMR ($CDCl_3$, 400 MHz): δ (ppm) 2.77-2.83 (m, 1H), 2.89-2.97 (m, 2H), 3.02-3.15 (m, 4H), 4.16 (ddt, *J* = 9.9, 2.1, 1.1 Hz, 1H) 6.45-6.53 (m, 5H), 6.81 (dd, *J* = 7.7, 2.0 Hz, 1H), 7.24 (d, *J* = 2.0 Hz, 1H).

3.10 Synthesis [2.2] paracyclophane carboxaldehyde

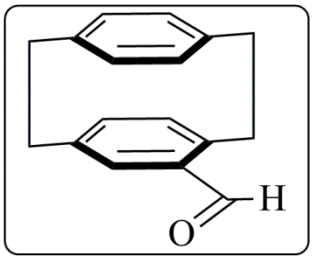

Based on literature [40], 1.0 g (4.8 mmol) of [2.2]paracyclophane was dissolved in DCM (50 mL) at 0 °C. 10 mL of $TiCl_4$ solution (1 M of solution in DCM) and 450 µL (5.00 mmol) of dichloromethoxymethane were added consequently. The reaction mixture was stirred overnight under nitrogen atmosphere and the color turned to blue. 50 mL of water was added to the solution and obtained two phases. The color of organic

phase turned to green. The mixture was extracted with DCM three times and organic phase was then dried with anhydrous salt, filtrated and the solvent was evaporated using rotary evaporator and obtained brownish solid. The brown solid was then purified by flash column chromatography (EtOAc:Hexane = 1:5, Rf = 0.8) on silica gel and obtained 700 mg (2.96 mmol) of white solid. Yield is 68%.

^{1}H NMR ($CDCl_3$, 400 MHz): δ (ppm) 2.79-2.84 (m, 1H), 2.94 (m, 1H), 2.99-3.16 (m, 6H), 4.15 (ddt, *J* = 9.8, 2.1, 1.0 Hz, 1H) 6.46-6.54 (m, 5H), 6.72 (dd, 7.8, 2.1 Hz, 1H), 7.27 (d, *J* = 1.9 Hz, 1H), 9.95 (1H, s).

3.11 Synthesis [2.2] paracyclophane-2-carboxylic with hydrogen peroxide

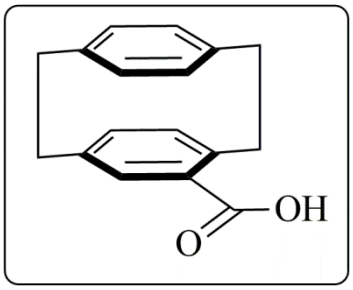

Based on literature [41], 600 mg (2.54 mmol) of [2.2]paracyclophane carboxaldehyde was dissolved in methanol (10 mL). 1.2 mL of 50% potassium hydroxide solution was added and the mixture was heated to 65 °C. 2 mL of 50% hydrogen peroxide solution was added dropwise and the mixture turned to white from colorless. The reaction mixture was stirred overnight and cooled down to room temperature. 1 M of HCl solution was added until the solution was acidic. The mixture was extracted with DCM six times and organic phase was then dried over anhydrous Na_2SO_4, filtrated and the solvent was evaporated using rotary evaporator and obtained yellow solid. The solid was then purified by flash column chromatography (EtOAc:Hexane = 1:4, Rf = 0.4) on silica gel and obtained 190 mg (0.753 mmol) of white solid. Yield is 30%.

^{1}H NMR ($CDCl_3$, 400 MHz): δ (ppm) 2.77-2.83 (m, 1H), 2.89-2.97 (m, 2H), 3.02-3.15 (m, 4H), 4.16 (ddt, *J* = 9.9, 2.1, 1.1 Hz, 1H) 6.45-6.53 (m, 5H), 6.81 (dd, *J* = 7.7, 2.0 Hz, 1H), 7.24 (d, *J* = 2.0 Hz, 1H).

3.12 Synthesis [2.2] paracyclophane-2-carboxylic with $KMnO_4$

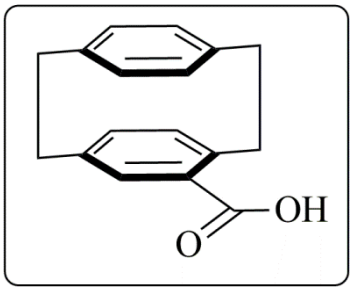

Based on literature [38], 250 mg (1.06 mmol) [2.2]paracyclophane carboxaldehyde was dissolved in acetone (20 mL) at 0 °C. 550 mg (3.48 mmol) of $KMnO_4$ in 2 mL of water was added to this solution and stirred for 2 hours. After 2 hours, 20% (w/v) NaOH solution (2 mL) was added and stirred for 15 minutes at room temperature. Additional (10%) NaOH solution (2 mL) was added. The mixture was filtrated and yellowish solid was obtained. The filtrate was extracted three times with diethyl ether to remove the remaining [2.2]paracyclophane carboxaldehyde. 1 M HCl was added until the pH of the solution was 4 and the solution was extracted five times with diethyl ether. Organic phase was then dried over anhydrous $MgSO_4$, filtrated and the solvent was evaporated using rotary evaporator and obtained 240 mg (0.952 mmol) of white solid. Yield is 89%.

^{1}H NMR ($CDCl_3$, 400 MHz): δ (ppm) 2.77-2.83 (m, 1H), 2.89-2.97 (m, 2H), 3.02-3.15 (m, 4H), 4.16 (ddt, *J* = 9.9, 2.1, 1.1 Hz, 1H) 6.45-6.53 (m, 5H), 6.81 (dd, *J* = 7.7, 2.0 Hz, 1H), 7.24 (d, *J* = 2.0 Hz, 1H).

3.13 Synthesis of [2.2] paracyclophanoyl phenylalanine methyl ester

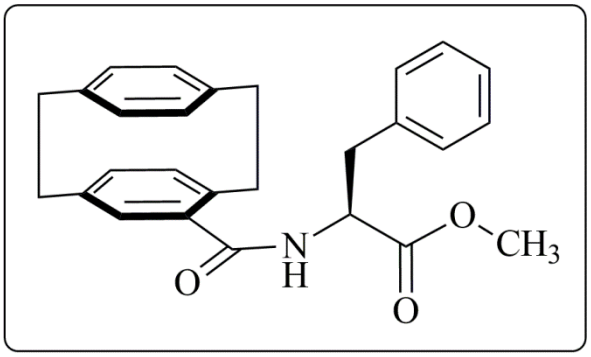

Based on literature [20], 100 mg (0.397 mmol) of [2.2]paracyclophane-2-carboxylic acid, 200 mg (0.58 mmol) of HBTU and 100 mg (0.74 mmol) of anhydrous HOBt were dissolved in DCM (50 mL) at 0 °C. To activate carbonyl group, 190 mL (1.30 mmol) of triethylamine (Et_3N) was

added subsequently for 1 hour to the stirred reaction mixture. After 1 hour, 1 equivalent (120 mg, 0.40 mmol) of L-phenylalanine methyl ester salt was added and the reaction mixture was stirred for 3 days. The reaction mixture was then washed with Na_2CO_3, HCl and extracted with DCM three times. Organic phase was then dried over anhydrous Na_2SO_4, filtrated and the solvent was evaporated using rotary evaporator and obtained a yellowish white solid. The solid was then purified by flash column chromatography (EtOAc:Hexane = 1:1) on silica gel and obtained 70 mg (0.16 mmol) of yellowish solid. Yield is 41%.

^{1}H NMR ($CDCl_3$, 400 MHz): δ (ppm) 2.82 (m, 2H), 2.90-3.15 (m, 8H), 3.75 (s, 3H), 4.86 (dd, *J* = 7.5, 2.3 Hz, 1H) 6.45-6.53 (m, 5H), 6.74 (dd, *J* = 8.0, 2.1 Hz, 1H), 6.95 (m, 1H), 7.27-7.33 (m, 3H), 7.38 (d, *J* = 2.0 Hz, 2H).

3.14 Synthesis of [2.2] paracyclophanoyl phenylalanine

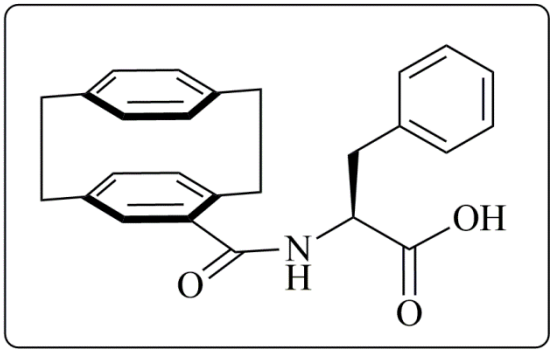

Based on literature [20], 120 mg (0.290 mmol) of [2.2]paracyclophane phenylalanine methyl ester was dissolved in methanol (45 mL). 1 M NaOH solution (20 mL) was added and stirred for 5 hours. The reaction mixture was neutralized with 1 M of HCl solution and evaporated under low pressure using rotary evaporator to remove methanol from the solution. The aqueous mixture was then acidified with 1 M HCl solution. The acidic solution was extracted with DCM four times. Organic phase was then dried, filtrated and the solvent was evaporated using rotary evaporator and obtained a brownish solid. The solid was then purified by flash column chromatography using EtOAc on silica gel and obtained 100 mg of white solid and dissolved in 4 mL of CH_3CN and 4 mL of deionized water and dried in freeze dryer for overnight. 85 mg (0.22 mmol) of white solid was obtained. Yield is 77%.

^{1}H NMR ($CDCl_3$, 400 MHz): δ (ppm) 2.73-3.04 (m, 5H), 3.08-3.27 (m, 3H), 3.32-3.46 (m, 1.5H), 3.65 (ddd, *J* = 12.67, 10.18, 2.11 Hz, 0.5H), 5.00-5.11 (m, 1H),

5.92-6.05 (m, 1H), 6.21-6.31 (m, 1H), 6.40-6.53 (m, 3H), 6.55-6.63 (m, 2H), 7.28-7.42 (m, 5H).

^{13}C NMR ($CDCl_3$, 100 MHz): δ (ppm) 31.4, 35.2, 35.4, 35.5, 36.8, 58.8, 124.6, 125.8, 126.3, 126.8, 127.1, 127.2, 127.9, 128.4, 130.8, 131.2, 131.3, 131.6, 135.1, 135.3, 136.0, 136.4, 138.4, 138.6, 166.7, 179.4.

HRMS $C_{26}H_{25}NO_3$ $[M-H]^+$: Calculated 400.1913, found 400.1914.

3.15 Synthesis of [2.2] paracyclophanoyl tyrosine

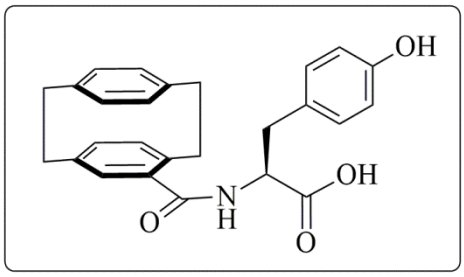

For the synthesis of [2.2]paracyclophanoyl tyrosine, general procedure of solid phase peptide synthesis was applied starting with 0.1 mmol of 2-chlorotrityl chloride resin. 250 mg (0.55 mmol) of Fmoc-*O*-*tert*-butyl-L-tyrosine and 76 mg (0.30 mmol) of [2.2] paracyclophane-2-carboxylic acid were used and obtained 38 mg (0.091 mmol) of **PC-Y** compound with 91% yield.

^{1}H NMR ($CDCl_3$, 400 MHz): δ (ppm) 2.89-3.12 (m, 8H), 3.20-3.30 (m, 1H), 3.32-3.40 (m, 0.5H), 3.52-3.65 (m, 0.5H), 4.84-4.90 (m, 1H), 6.21-6.26 (m, 1H), 6.37-6.45 (m, 3H), 6.48-6.58 (m, 2H), 6.75 (t, J = 8.60 Hz, 2H), 7.02-7.09 (m, 2H), 7.20-7.23 (m, 1H).

^{13}C NMR ($CDCl_3$, 100 MHz): δ (ppm) 30.7, 33.2, 34.4, 34.7, 36.2, 53.6, 116.6, 117.4, 125.9, 126.2, 127.1, 127.8, 128.3, 130.8, 131.5, 131.3, 132.3, 135.2, 135.4, 136.5, 137.1, 138.2, 138.6, 155.8, 165.4, 181.4.

HRMS $C_{26}H_{25}NO_4$ $[M-H]^+$: Calculated 416.1862, found 416.1868.

3.16 Synthesis of [2.2] paracyclophanoyl tryptophan

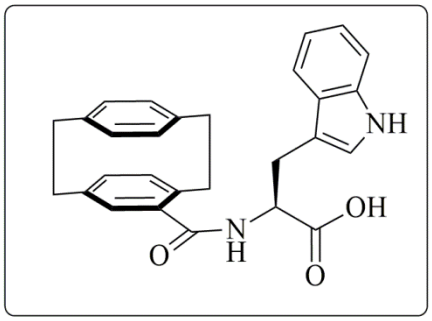

For the synthesis of [2.2]paracyclophanoyl tyrosine, general procedure of solid phase peptide synthesis was applied starting with 0.1 mmol of 2-chlorotrityl chloride resin. 290 mg (0.55 mmol) of $N_{(in)}$-Boc-N_{α}-Fmoc-L-tryptophan and 75 mg (0.30 mmol) of [2.2] paracyclophane-2-carboxylic acid were used and obtained 41 mg (0.093 mmol) of **PC-W** compound with 93% yield.

^{1}H NMR ($CDCl_3$, 400 MHz): δ (ppm) 2.60-2.95 (m, 7H), 3.32-3.58 (m, 3H), 4.95-5.05 (m, 1H), 5.92-6.03 (m, 1H), 6.09-6.16 (m, 1H), 6.28-6.40 (m, 4H), 6.42-6.47 (m, 1H), 7.11-7.16 (m, 1H), 7.23-7.26 (m, 1H), 7.35 (dd, J = 7.56, 6.64 Hz, 1H), 7.62-7.70 (m, 1H), 8.12-8.28 (m, 1H).

^{13}C NMR ($CDCl_3$, 100 MHz): δ (ppm) 30.1, 32.3, 34.7, 34.9, 35.4, 54.2, 113.6, 114.5, 121.2, 121.5, 122.0, 122.2, 127.6, 127.8, 128.2, 128.4, 131.3, 131.7, 131.8, 132.5, 134.9, 135.2, 135.6, 135.8, 138.4, 139.2, 170.8, 181.6.

HRMS $C_{28}H_{26}N_2O_3$ $[M-H]^+$: Calculated 439.2022, found 439.2033.

3.17 Synthesis of [2.2] paracyclophanoyl phenylalanine aspartic acid

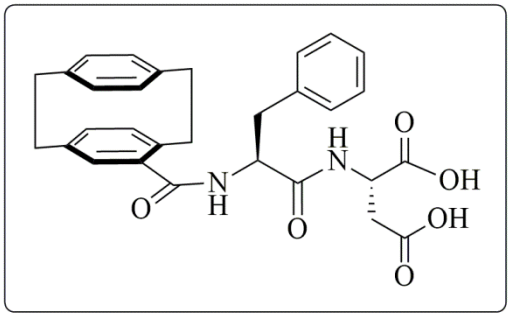

For the synthesis of [2.2] paracyclophanoyl phenylalanine aspartic acid, general procedure of solid phase peptide synthesis was applied starting with 0.05 mmol of 2-chlorotrityl chloride resin. 113 mg (0.275 mmol) of Fmoc-L-aspartic acid 4-*tert*-butyl ester, 107 mg (0.275 mmol) of Fmoc-L-phenylalanine and 50 mg (0.20 mmol) of [2.2] paracyclophane-2-carboxylic acid were used and obtained 24 mg (0.047 mmol) of **PC-F-D** compound with 94% yield.

HRMS $C_{30}H_{30}N_2O_6$ $[M-H]^+$: Calculated 514.2342, found 514.2260.

3.18 Synthesis of [2.2]paracyclophanoyl phenylalanine glutamic acid

For the synthesis of [2.2]paracyclophanoyl phenylalanine glutamic acid, general procedure of solid phase peptide synthesis was applied starting with 0.05 mmol of 2-chlorotrityl chloride resin. 117 mg (0.275 mmol) of Fmoc-L-glutamic acid 5-*tert*-butyl ester, 107 mg (0.275 mmol) of Fmoc-L-phenylalanine and 50 mg (0.20 mmol) of [2.2] paracyclophane-2-carboxylic acid were used and obtained 24 mg (0.045 mmol) of **PC-F-E** compound with 90% yield.

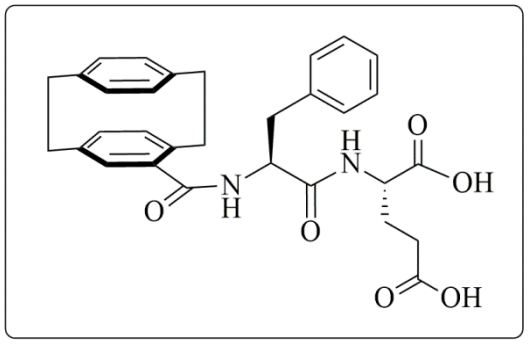

HRMS $C_{31}H_{32}N_2O_6$ $[M-H]^+$: Calculated 528.2498, found 528.2474.

3.19 Synthesis of [2.2] paracyclophanoyl phenylalanine arginine

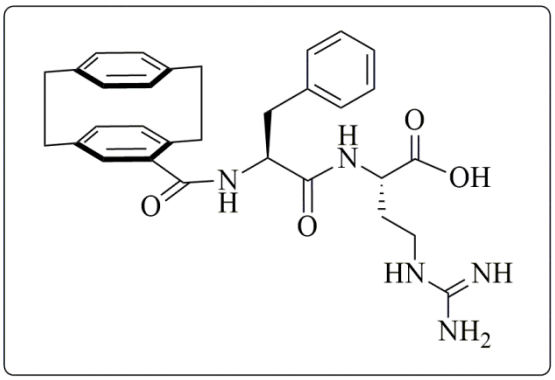

For the synthesis of [2.2] paracyclophanoyl phenylalanine arginine, general procedure of solid phase peptide synthesis was applied starting with 0.05 mmol of 2-chlorotrityl chloride resin. 180 mg (0.275 mmol) of N_{α}-Fmoc-N_{ω}-Pbf-L-arginine, 107 mg (0.275 mmol) of Fmoc-L-phenylalanine and 50 mg (0.20 mmol) of [2.2] paracyclophane-2-carboxylic acid were used and obtained 25 mg (0.046 mmol) of **PC-F-R** compound with 91% yield.

HRMS $C_{32}H_{37}N_5O_4$ $[M-H]^+$: Calculated 555.2927, found 555.2980.

3.20 Synthesis of [2.2]paracyclophanoyl tyrosine aspartic acid

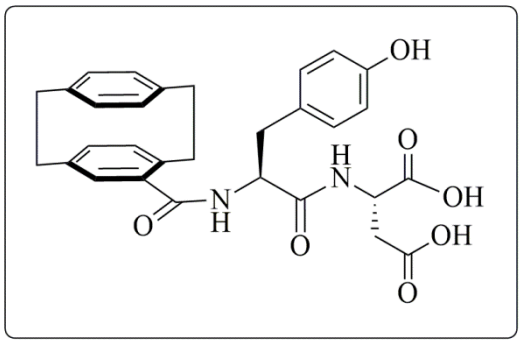

For the synthesis of [2.2]paracyclophanoyl tyrosine aspartic acid, general procedure of solid phase peptide synthesis was applied starting with 0.05 mmol of 2-chlorotrityl chloride resin. 113 mg (0.275 mmol) of Fmoc-L-aspartic acid 4-*tert*-butyl ester, 126 mg (0.275 mmol) of Fmoc-*O*-*tert*-butyl-L-tyrosine and 50 mg (0.20 mmol) of [2.2] paracyclophane-2-carboxylic acid were used and obtained 25 mg (0.048 mmol) of **PC-Y-D** compound with 95% yield..

HRMS $C_{30}H_{30}N_2O_7$ $[M-H]^+$: Calculated 531.2131, found 531.2124.

3.21 Synthesis of [2.2] paracyclophanoyl tyrosine glutamic acid

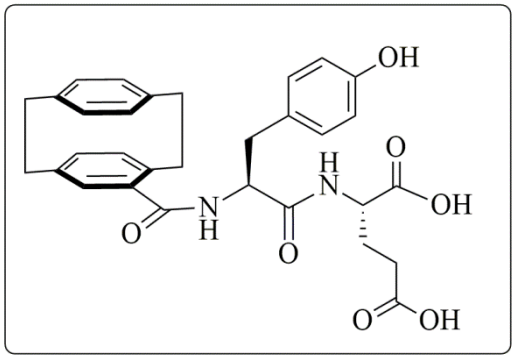

For the synthesis of [2.2] paracyclophanoyl tyrosine glutamic acid, general procedure of solid phase peptide synthesis was applied starting with 0.05 mmol of 2-chlorotrityl chloride resin. 117 mg (0.275 mmol) of Fmoc-L-glutamic acid 5-*tert*-butyl ester, 126 mg (0.275 mmol) of Fmoc-*O*-*tert*-butyl-L-tyrosine and 50 mg (0.20 mmol) of [2.2] paracyclophane-2-carboxylic acid were used and obtained 25 mg (0.047 mmol) of **PC-Y-E** compound with 93% yield

HRMS $C_{31}H_{32}N_2O_7$ $[M-H]^+$: Calculated 545.2288, found 545.2289.

3.22 Synthesis of [2.2] paracyclophanoyl tyrosine arginine

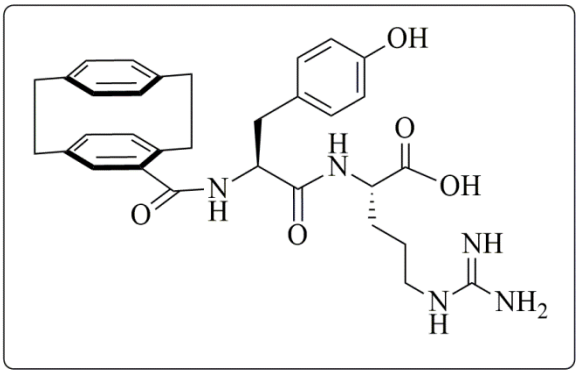

For the synthesis of [2.2] paracyclophanoyl tyrosine arginine, general procedure of solid phase peptide synthesis was applied starting with 0.05 mmol of 2-chlorotrityl chloride resin. 180 mg (0.275 mmol) of N_α-Fmoc-N_ω-Pbf-L-arginine, 126 mg (0.275 mmol) of Fmoc-*O*-*tert*-butyl-L-tyrosine and 50 mg (0.20 mmol) of [2.2] paracyclophane-2-carboxylic acid were used and obtained 25 mg (0.044 mmol) of **PC-Y-R** compound with 88% yield.

HRMS $C_{32}H_{37}N_5O_5$ $[M-H]^+$: Calculated 572.2873, found 572.2857.

3.23 Synthesis of [2.2] paracyclophanoyl tryptophan aspartic acid

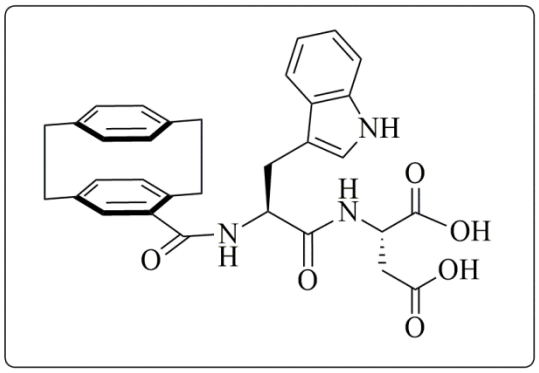

For the synthesis of [2.2] paracyclophanoyl tryptophan aspartic acid, general procedure of solid phase peptide synthesis was applied starting with 0.05 mmol of 2-chlorotrityl chloride resin. 113 mg (0.275 mmol) of Fmoc-L-aspartic acid 4-*tert*-butyl ester, 145 mg (0.275 mmol) of $N_{(in)}$-Boc-N_{α}-Fmoc-L-tryptophan and 50 mg (0.20 mmol) of [2.2] paracyclophane-2-carboxylic acid were used and obtained 25 mg (0.046 mmol) of **PC-W-D** compound with 92% yield.

HRMS $C_{32}H_{31}N_3O_6$ $[M-H]^+$: Calculated 554.2291, found 554.2275.

3.24 Synthesis of [2.2] paracyclophanoyl tryptophan glutamic acid

For the synthesis of [2.2] paracyclophanoyl tryptophan glutamic acid, general procedure of solid phase peptide synthesis was applied starting with 0.05 mmol of 2-chlorotrityl chloride resin. 117 mg (0.275 mmol) of Fmoc-L-glutamic acid 5-*tert*-butyl ester, 145 mg (0.275 mmol) of $N_{(in)}$-Boc-N_{α}-Fmoc-L-tryptophan and 50 mg (0.20 mmol) of [2.2] paracyclophane-2-carboxylic acid were used and obtained 27 mg (0.047 mmol) of **PC-W-E** compound with 94% yield.

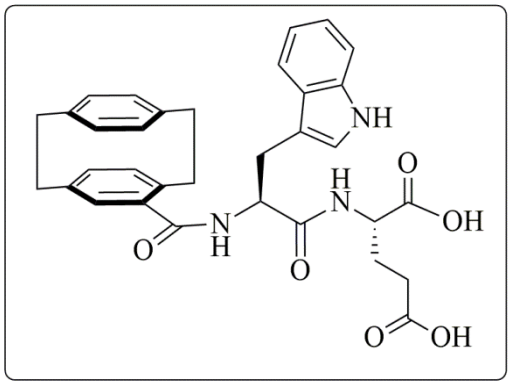

HRMS $C_{33}H_{33}N_3O_6$ $[M-H]^+$: Calculated 568.2448, found 568.2455.

3.25 Synthesis of [2.2] paracyclophanoyl tryptophan arginine

For the synthesis of [2.2] paracyclophanoyl tryptophan arginine, general procedure of solid phase peptide synthesis was applied starting with 0.05 mmol of 2-chlorotrityl chloride resin. 180 mg (0.275 mmol) of N_{α}-Fmoc-N_{ω}-Pbf-L-arginine, 145 mg (0.275 mmol) of $N_{(in)}$-Boc-N_{α}-Fmoc-L-tryptophan and 50 mg (0.20 mmol) of [2.2] paracyclophane-2-carboxylic acid were used and obtained 26 mg (0.045 mmol) of **PC-W-R** compound with 89% yield.

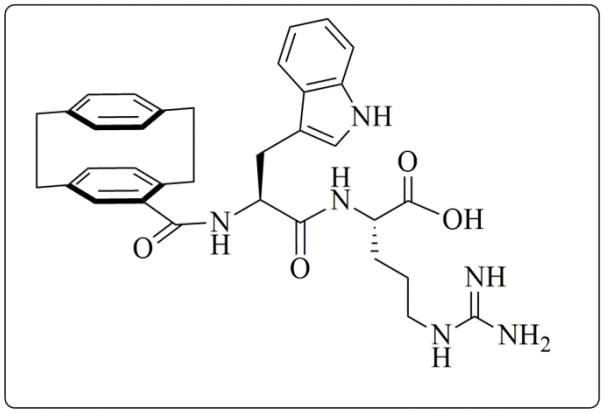

HRMS $C_{34}H_{38}N_6O_4$ $[M-H]^+$: Calculated 595.3033, found 595.3033.

3.26 Resolution of [2.2] paracyclophane-2-carboxylic acid

Based on literature [39], 550 mg of racemic [2.2] paracyclophane-2-carboxylic acid and 290 mg of (*S*)-(-)-α-methylbenzylamine were dissolved in 20 mL of $CHCl_3$ and stirred for 1 hour at room temperature. Then, 20 mL of diethyl ether was added to this solution and placed in an ice bath for 48 hours. The solution then was filtrated. The organic solvent of the filtrate was evaporated under vacuum and 710 mg of yellow solid was obtained. 12 mL of cold ethanol was added to this solid and allowed to precipitate in an ice bath. The precipitate and the filtrate were separated.

The precipitate was dissolved in 10 mL of $CHCl_3$. 5 mL of dilute hydrochloric acid solution was added to the solution and stirred for 30 minutes at room temperature. The organic layer was then separated and extracted with 1 M of NaOH solution. The aqueous phase was then acidified and extracted with $CHCl_3$. Organic layer

was dried under vacuum and obtained 110 mg of (*R*)-[2.2] paracyclophane-2-carboxylic acid.

The solvent of the filtrate was evaporated under vacuum and the same procedure described above was applied. 125 mg of (*S*)-[2.2] paracyclophane-2-carboxylic acid was obtained.

Optical rotation of (*S*)-(+)-[2.2] paracyclophane-2-carboxylic acid was found as $[\alpha]_D = +162^\circ$ (c = 1.0 x 10^{-2} g/mL, $CHCl_3$) where lit. $[\alpha]_D = +162^\circ$.

Optical rotation of (*R*)-(-)-[2.2] paracyclophane-2-carboxylic acid was found as $[\alpha]_D = -153^\circ$ (c = 1.0 x 10^{-2} g/mL, $CHCl_3$) where lit. $[\alpha]_D = -157^\circ$

REFERENCES

1) Zhang, S. Emerging biological materials through molecular self-assembly. *Biotechnol. Adv*. **2002**, *20*, 321-339.

2) Zhang, S. Fabrication of novel biomaterials through molecular self-assembly. *Nat. Biotechnol*. **2003,** *21*, 1171-1178.

3) Whitesides, G. M.; Grzybowski, B. Self-assembly at all scales. *Science*. **2002,** *295*, 2418-2421.

4) Raeburn, J.; Cardoso, A. Z.; Adams, D. J. The importance of the self-assembly process to control mechanical properties of low molecular weight hydrogels. *Chem. Soc. Rev*. **2013,** *42*, 5143-5156.

5) Aggeli, A.; Bell, M.; Boden, N.; Keen, J. N. Responsive gels formed by the spontaneous self-assembly of peptides into polymeric beta-sheet tapes. *Nature*. **1997,** *386*, 259-262.

6) Van Vlierberghe, S.; Dubruel, P.; Schacht, E. Biopolymer-based hydrogels as scaffolds for tissue engineering applications: a review. *Biomacromolecules*, **2011,** *12*, 1387-1408.

7) Flory, P. J., *Faraday Discuss. Chem. Soc.*, **1974**, *57*, 7–18.

8) Tomasini, C.; Castellucci, N. Peptides and peptidomimetics that behave as low molecular weight gelators. *Chem. Soc. Rev.*, **2013,** *42*, 156-172.

9) Nagai, Y.; Yokoi, H.; Kaihara, K.; Naruse, K., *Biomaterials*, **2012,** *33*, 1044-1051.

10) Smith, A. M.; Williams, R. J.; Tang, C.; Coppo, P.; Collins, R. F.; Turner, M. L.; Saiani, A.; Ulijn, R. V. Fmoc- Diphenylalanine Self Assembles to a Hydrogel via a Novel Architecture Based on π–π Interlocked β-Sheets. *Adv. Mater*. **2008,** *20*, 37-41.

11) Diegelmann, S. R.; Gorham, J. M.; Tovar, J. D. One-dimensional optoelectronic nanostructures derived from the aqueous self-assembly of π-conjugated oligopeptides. *J. Am. Chem. Soc.* **2008,** *130*, 13840-13841.

12) Stone, D. A., Tayi, A. S., Goldberger, J. E., Palmer, L. C., Stupp, S. I. Self-assembly and conductivity of hydrogen-bonded oligothiophene nanofiber networks. *Chem. Comm.* **2011,** *47*, 5702-5704.

13) Matson, J. B.; Zha, R. H.; Stupp, S. I. Peptide self-assembly for crafting functional biological materials. *Curr. Opin. Solid State Mater. Sci*. **2011,** *15*, 225-235.

14) Zelzer, M.; Ulijn, R. V. Next-generation peptide nanomaterials: molecular networks, interfaces and supramolecular functionality. *Chem. Soc. Rev*. **2011,** *39*, 3351-3357.

15) Wall, B. D.; Diegelmann, S. R.; Zhang, S.; Dawidczyk, T. J.; Wilson, W. L.; Katz, H. E.; Mao, H. Q.; Tovar, J. D. Aligned Macroscopic Domains of Optoelectronic Nanostructures Prepared via Shear- Flow Assembly of Peptide Hydrogels. *Adv. Mater*. **2011,** *23*, 5009-5014.

16) Brenzinger, K. Zur Kenntniss des Cystins und des Cystëins. (Mitgetheilt von E. Baumann.). *Z. Phys. Chem*. **1892,** *16*, 552-588.

17) de Loos, M.; Feringa, B. L.; van Esch, J. H. Design and application of self- assembled low molecular weight hydrogels. *Eur J. Org. Chem*. **2005,** *2005*, 3615-3631.

18) Tiller, J. C. Increasing the local concentration of drugs by hydrogel formation. *Angew. Chem. Int. Ed*. **2003,** *42*, 3072-3075.

19) Yang, Z.; Gu, H.; Zhang, Y.; Wang, L.; Xu, B. Small molecule hydrogels based on a class of antiinflammatory agents. *Chem. Commun*. **2004,** (2), 208-209.

20) Sun, Z., Li, Z., He, Y., Shen, R., Deng, L., Yang, M., Liang, Y., Zhang, Y. Ferrocenoyl phenylalanine: a new strategy toward supramolecular hydrogels with multistimuli responsive properties. *J. Am. Chem. Soc.*, ***2013,*** *135*, 13379-13386.

21) Ghini, G.; Lascialfari, L.; Vinattieri, C.; Cicchi, S.; Brandi, A.; Berti, D.; Betti, F.; Baglioni, P.; Mannini, M. Towards a general organogelator: combining a versatile scaffold and an efficient linking process. *Soft Matter*. **2009,** *5*, 1863-1869.

22) Afrasiabi, R.; Kraatz, H. B. Stimuli- Responsive Supramolecular Gelation in Ferrocene–Peptide Conjugates. *Chem. Eur. J*. **2013,** *19*, 17296-17300.

23) Bai, M.; Liang, J.; Xie, L.; Sanvito, S.; Mao, B.; Hou, S. Efficient conducting channels formed by the π-π stacking in single [2, 2] paracyclophane molecules. *J. Chem. Phys.*, **2012,** *136*, 104701.

24) Pierson, H. O. *Handbook of carbon, graphite, diamonds and fullerenes: processing, properties and applications*. **2012**, Noyes Publications, New Jersey.

25) Marrocchi, A.; Tomasi, I.; Vaccaro, L. Organic small molecules for photonics and electronics from the [2.2]paracyclophane scaffold. *Isr. J. Chem*. **2012,** *52*, 41-52.

26) Hollinger, J.; Jahnke, A. A.; Coombs, N.; Seferos, D. S. Controlling phase separation and optical properties in conjugated polymers through selenophene−thiophene copolymerization. *J. Am. Chem. Soc.,* **2010,** *132*, 8546-8547.

27) Tsuchiya, T.; Rudolf, M.; Wolfrum, S.; Radhakrishnan, S. G.; Aoyama, R.; Yokosawa, Y.; Oshima, A.; Akasaka, T.; Nagase, S.; Guldi, D. M. Coordinative interactions between porphyrins and C60, La@ C82, and La2@ C80. *Chem. Eur. J*., **2013,** *19*, 558-565.

28) Horowitz, G. Organic field-effect transistors. *Adv. Mater.*, **1998,** *10*, 365-377.

29) Edgar, L. J. Method and apparatus for controlling electric currents. U.S. Patent No: 1,745,175, **1930**.

30) Kahng, D.; Atalla, M. M. IRE solid-state devices research conference. *Carnegie Institute of Technology, Pittsburgh, PA*. **1960.**

31) Małachowski, M. J.; Żmija, J. Organic field-effect transistors. *Opto-Electron. Rev.* **2010,** *18*, 121-136.

32) Tsumura, A.; Koezuka, H.; Ando, T. Polythiophene field-effect transistor: Its characteristics and operation mechanism. *Synth. Metals*, **1988,** *25*, 11-23.

33) Aida, T.; Meijer, E. W.; Stupp, S. I. Functional supramolecular polymers. *Science*, **2012,** *335*, 813-817.

34) Tovar, J. D. Supramolecular construction of optoelectronic biomaterials. *Acc. Chem. Res.*, **2013,** *46*, 1527-1537.

35) Sanders, A. M.; Dawidczyk, T. J.; Katz, H. E.; Tovar, J. D. Peptide-based supramolecular semiconductor nanomaterials via Pd-catalyzed solid-phase "dimerizations". *ACS Macro Lett.*, **2012,** *1*, 1326-1329.

36) Kumar, R. J.; MacDonald, J. M.; Singh, T. B.; Waddington, L. J.; Holmes, A. B. Hierarchical self-assembly of semiconductor functionalized peptide α-helices and optoelectronic properties. *J. Am. Chem. Soc.*, **2011,** *133*, 8564-8573.

37) Sanders, A. M.; Kale, T. S.; Katz, H. E.; Tovar, J. D. Solid-phase synthesis of self-assembling multivalent π-conjugated peptides. *ACS Omega*, **2017,** *2*, 409-419.

38) Batsanov, A. S.; Hérault, D.; Howard, J. A.; Patrick, L. G.; Probert, M. R.; Whiting, A. Synthesis and structure of planar chiral, bifunctional aminoboronic acid ferrocene derivatives. *Organometallics*, **2007,** *26*, 2414-2419.

39) Kreis, M.; Nieger, M.; Bräse, S. Synthesis of novel planar-chiral [2.2] paracyclophane derivatives as potential ligands for asymmetric catalysis. *J. Organomet. Chem.*, **2006,** *691*, 2171-2181.

40) Rieche, A.; Gross, H.; Höft, E. Über α- Halogenäther, IV. Synthesen aromatischer Aldehyde mit Dichlormethyl- alkyläthern. *Chemische Berichte*, **1960,** *93*, 88-94.

41) Cong, Z. Q.; Wang, C. I.; Chen, T.; Yin, B. Z. Efficient and Rapid Method for the Oxidation of Electron- Rich Aromatic Aldehydes to Carboxylic Acids Using Improved Basic Hydrogen Peroxide. *Synth. Commun.*, **2006,** *36*, 679-683.

42) Marshall, J. L.; Hall, L. The electronic spectrum of (−)-s-(ps)-2, 5, 3', 6'-tetrahydro [2.2]paracyclophane-2-carboxylic acid. *Tetrahedron,* **1981,** *37*, 1271-1275.

APPENDIX A

NMR DATA

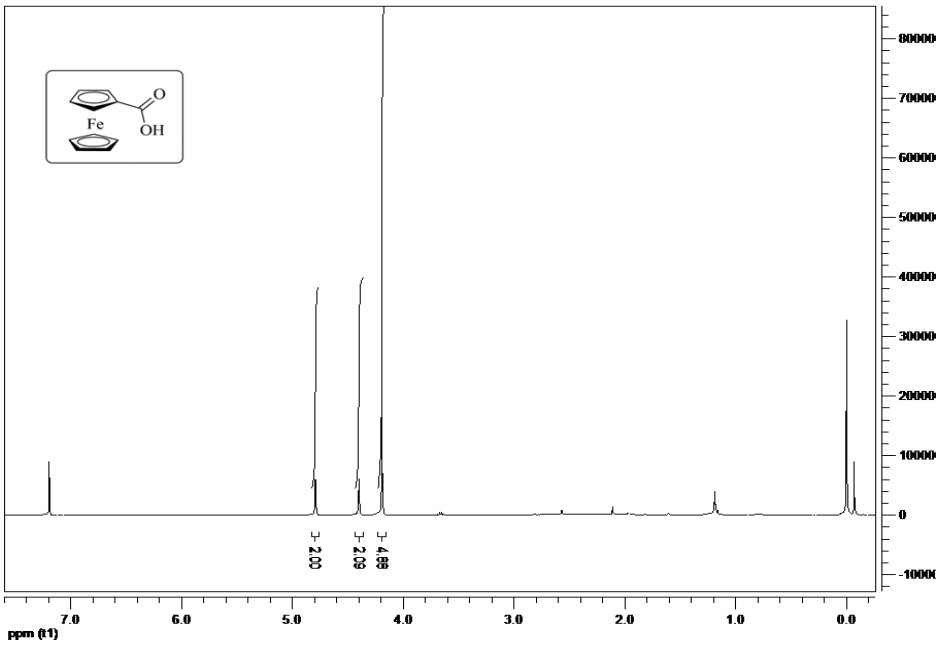

Figure A 1. ^{1}H NMR spectrum of ferrocenecarboxylic acid (**2**).

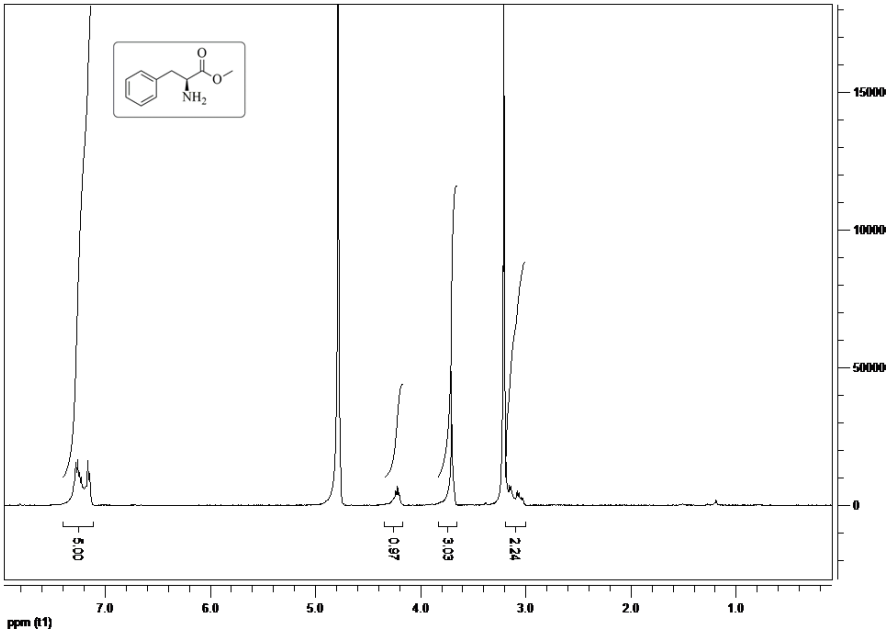

Figure A 2. ^{1}H NMR spectrum of L-phenylalanine methyl ester (**4**).

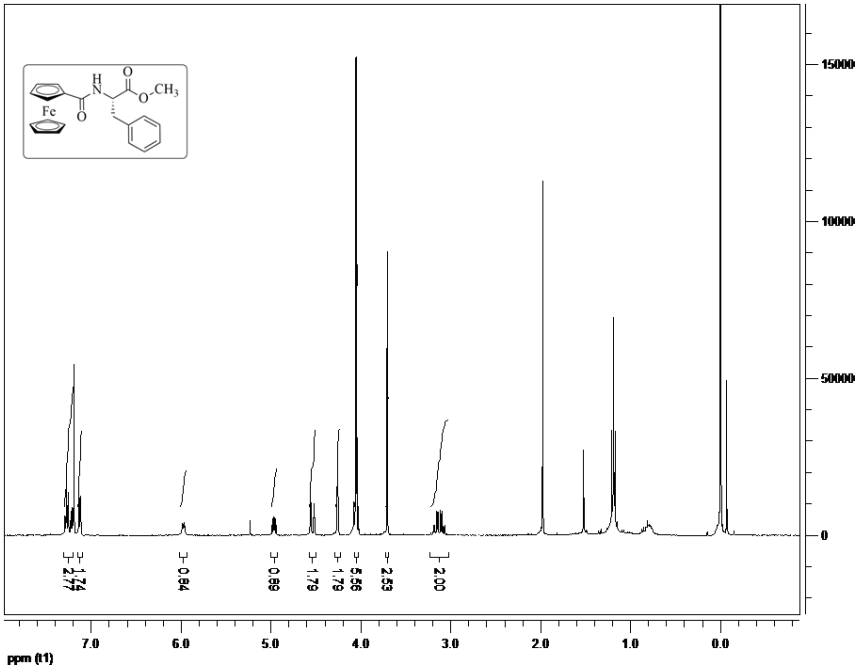

Figure A 3. ^{1}H NMR spectrum of ferrocenoyl phenylalanine methyl ester (**3**).

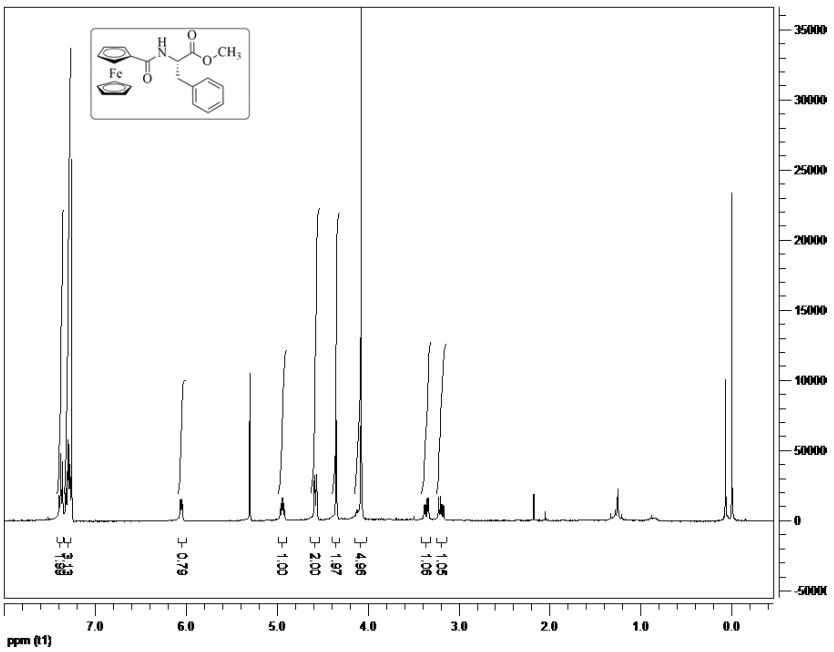

Figure A 4. [1]H NMR spectrum of ferrocenoyl phenylalanine (**5**).

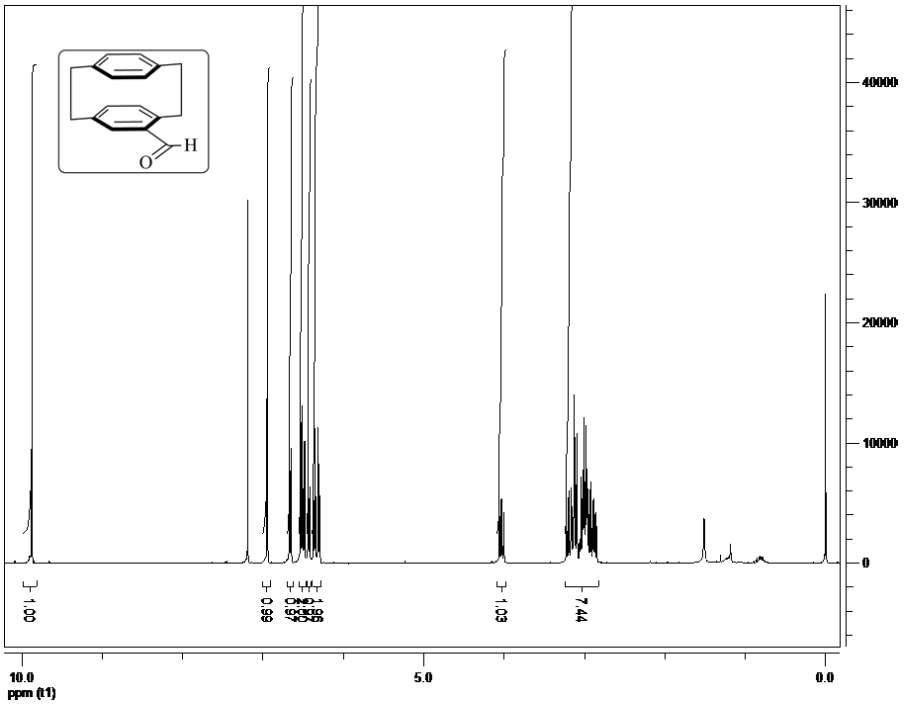

Figure A 5. [1]H NMR spectrum of [2.2] paracyclophane carboxaldehyde (**9**).

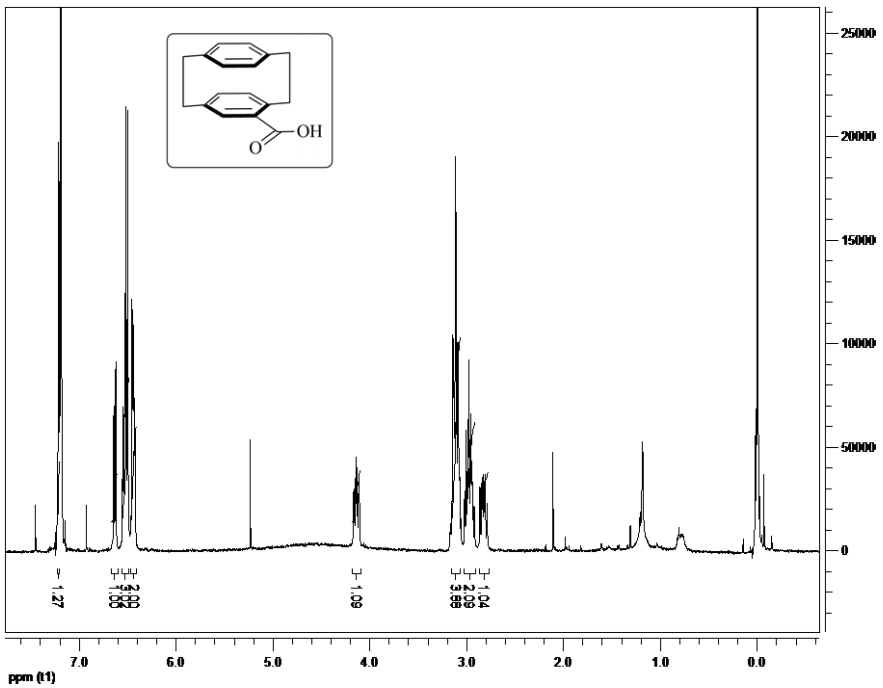

Figure A 6. ^{1}H NMR spectrum of [2.2] paracyclophane-2-carboxylic acid (**8**).

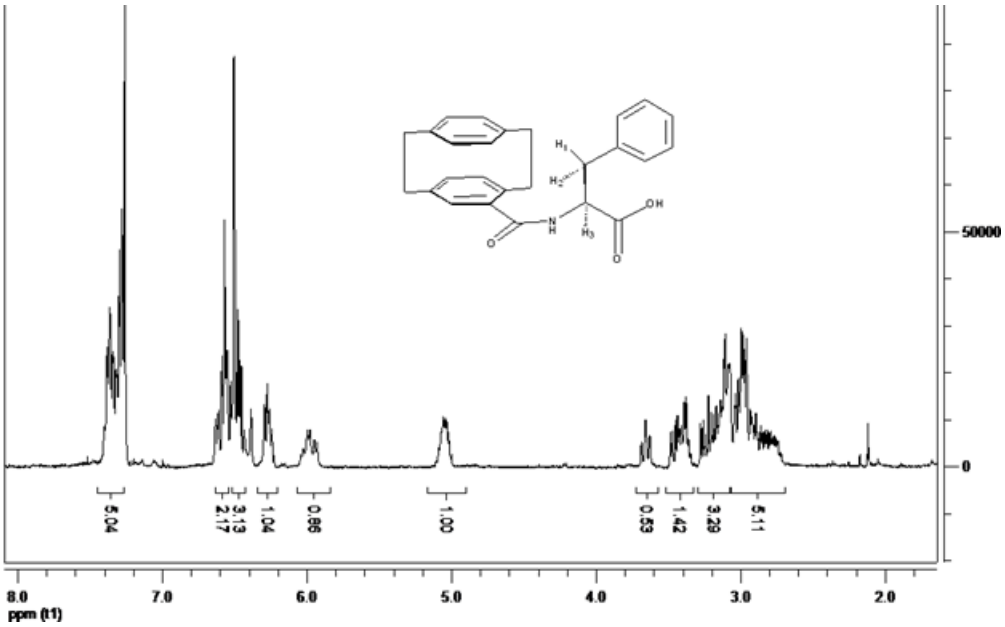

Figure A 7. ^{1}H NMR spectrum of [2.2] paracyclophanoyl phenylalanine (**11**).

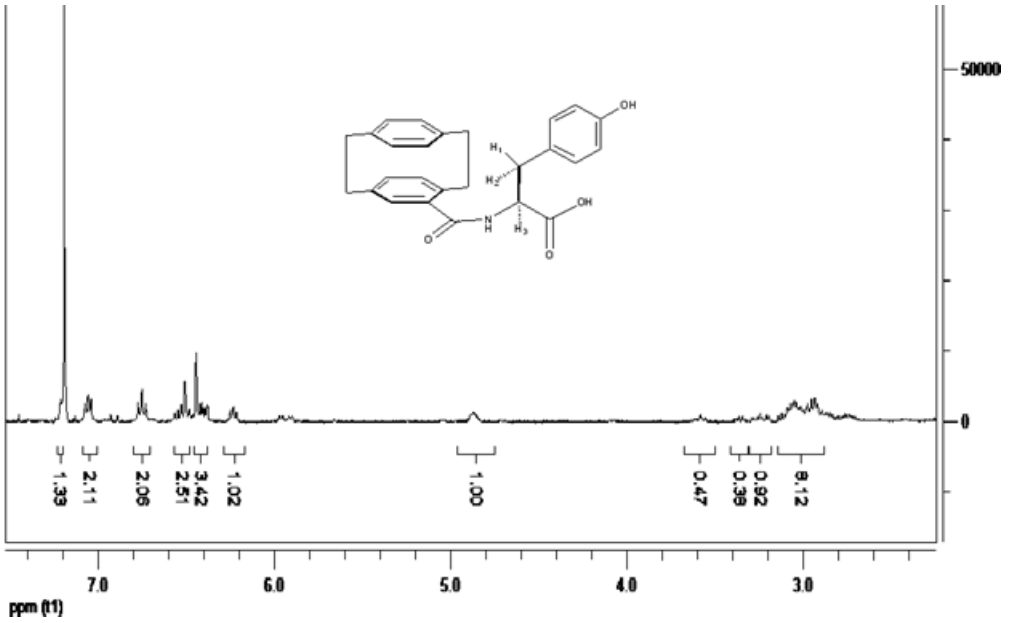

Figure A 8. [1]H NMR spectrum of [2.2] paracyclophanoyl tyrosine (**14**).

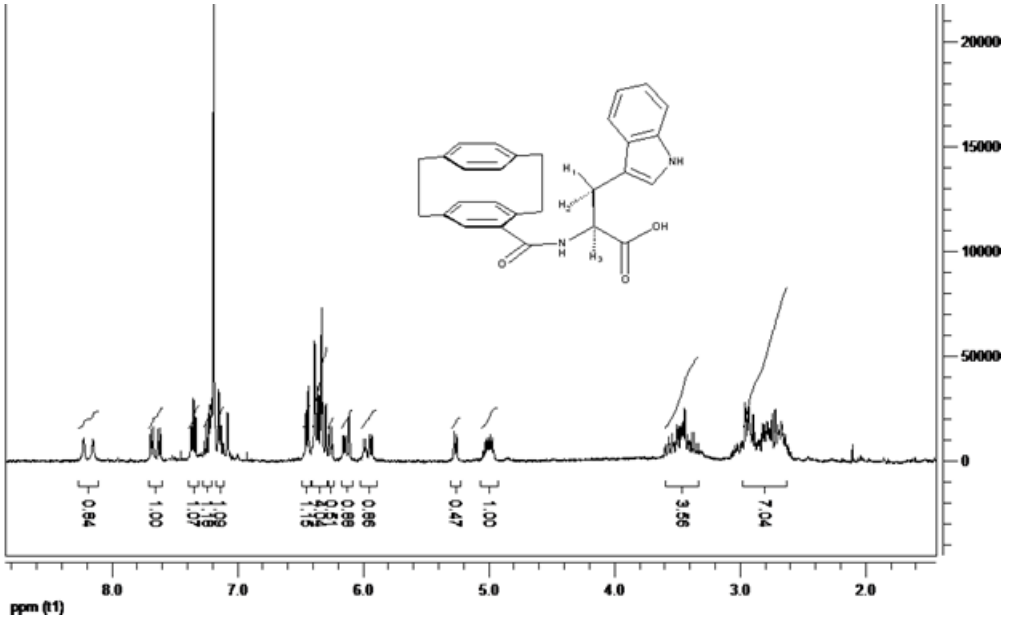

Figure A 9. [1]H NMR spectrum of [2.2] paracyclophanoyl tryptophan (**15**).

APPENDIX B

HPLC DATA

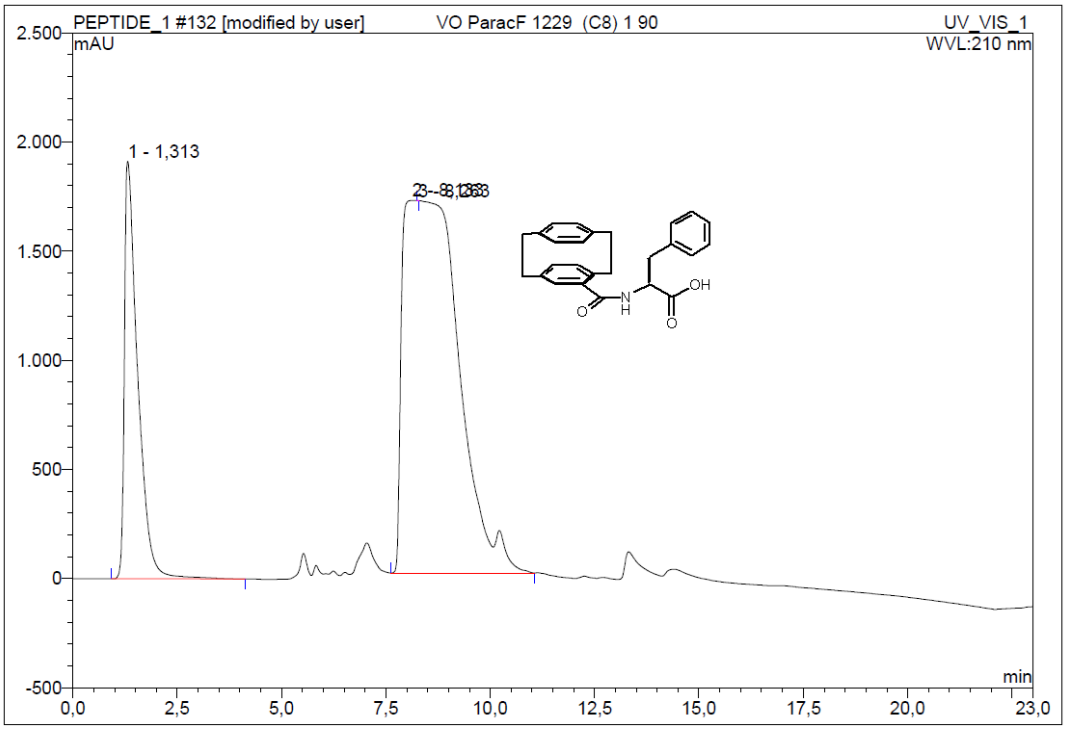

Figure B 1. HPLC chromatogram of [2.2] paracyclophanoyl phenylalanine (**11**).

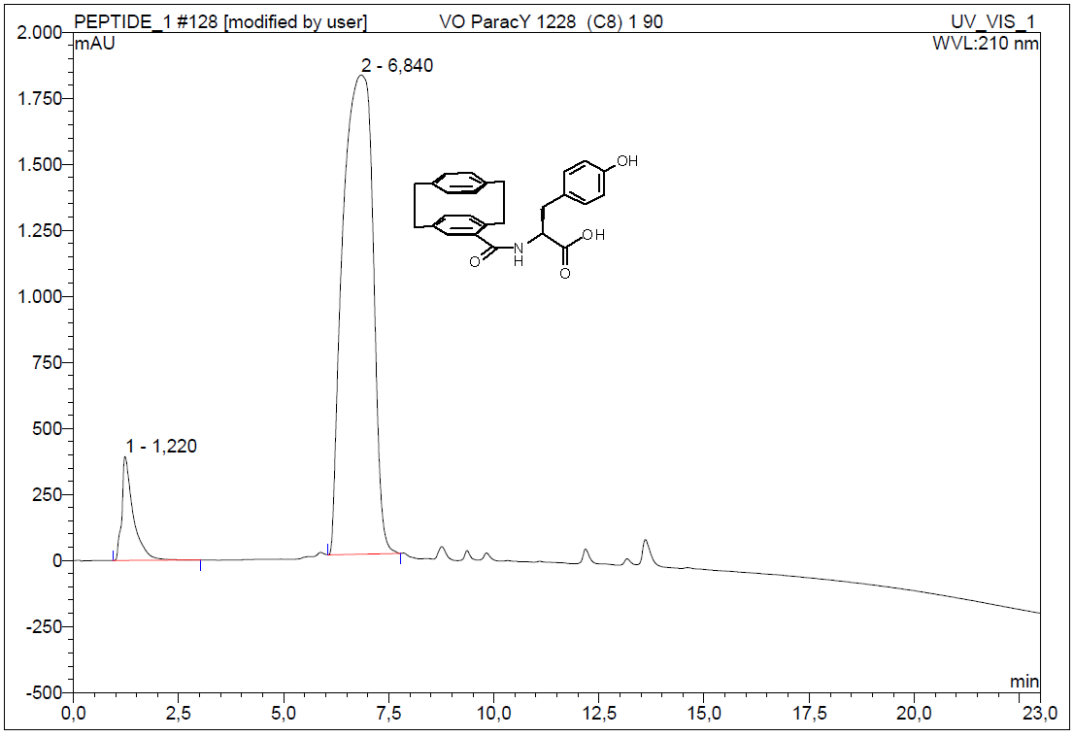

Figure B 2. HPLC chromatogram of [2.2] paracyclophanoyl tyrosine (**14**).

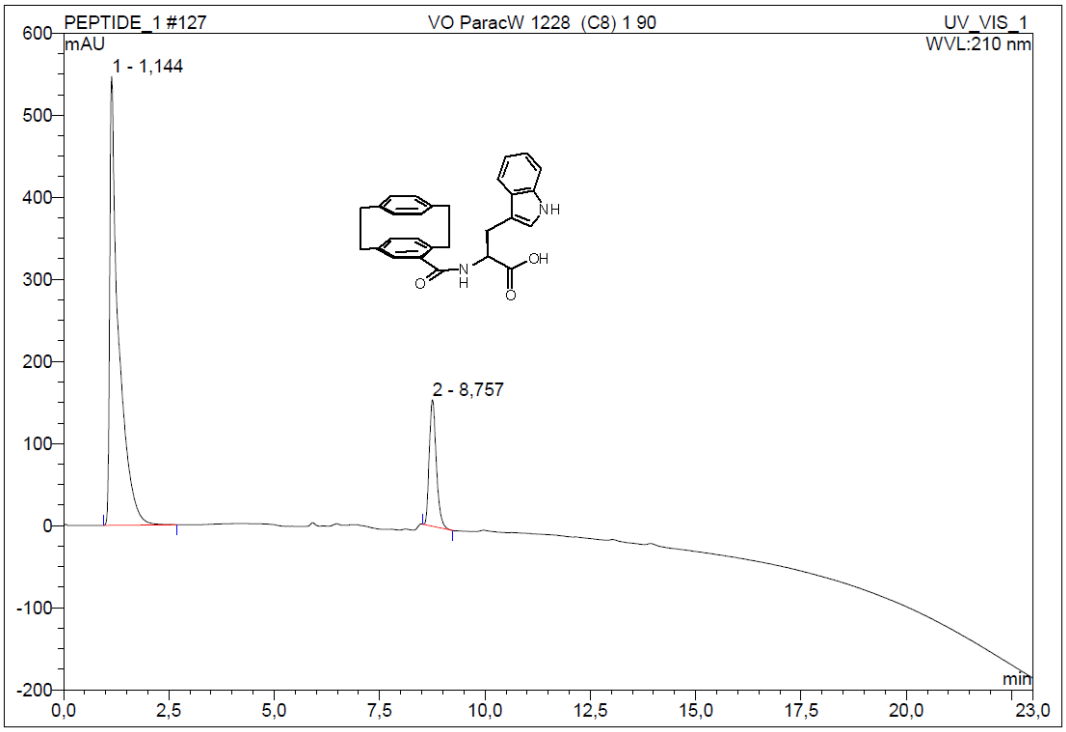

Figure B 3. HPLC chromatogram of [2.2] paracyclophanoyl tryptophan (**15**).

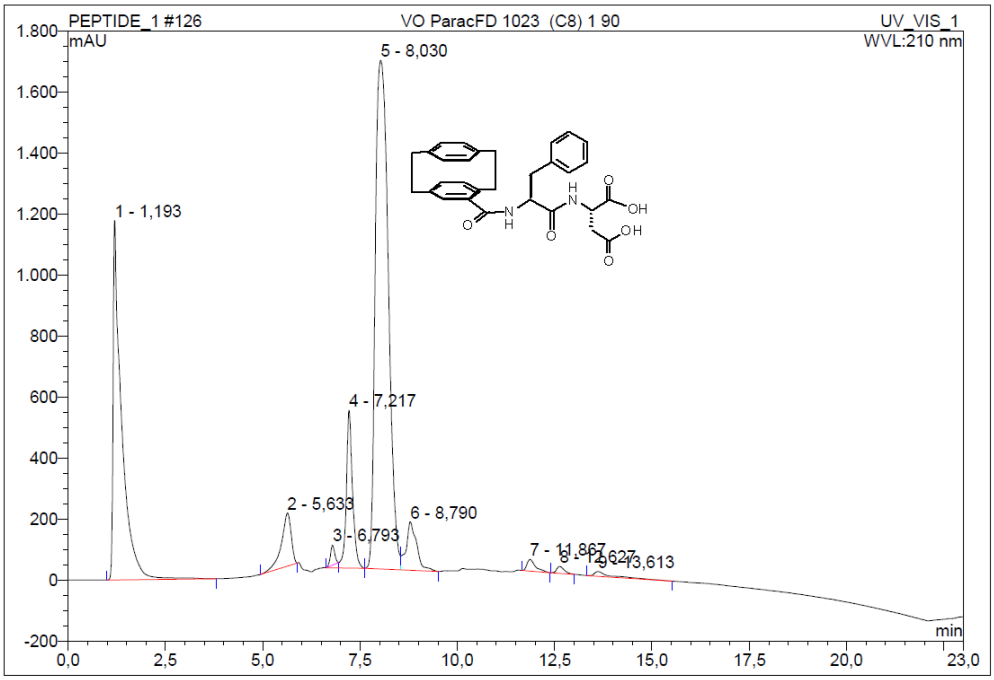

Figure B 4. HPLC chromatogram of [2.2] paracyclophanoyl phenylalanine aspartic acid (**16**).

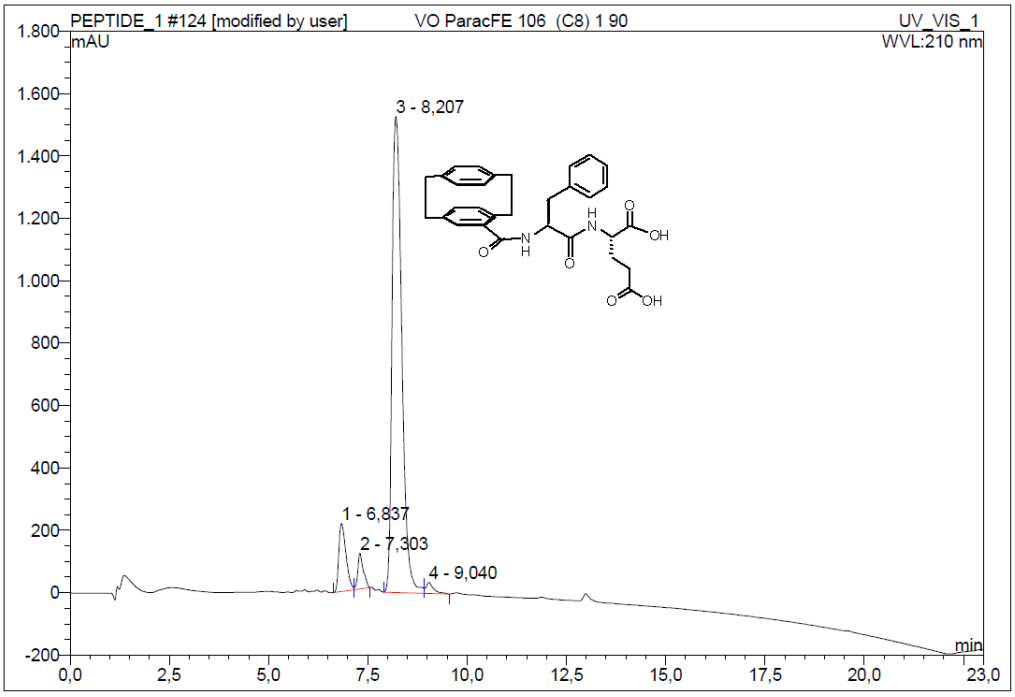

Figure B 5. HPLC chromatogram of [2.2] paracyclophanoyl phenylalanine glutamic acid (**17**).

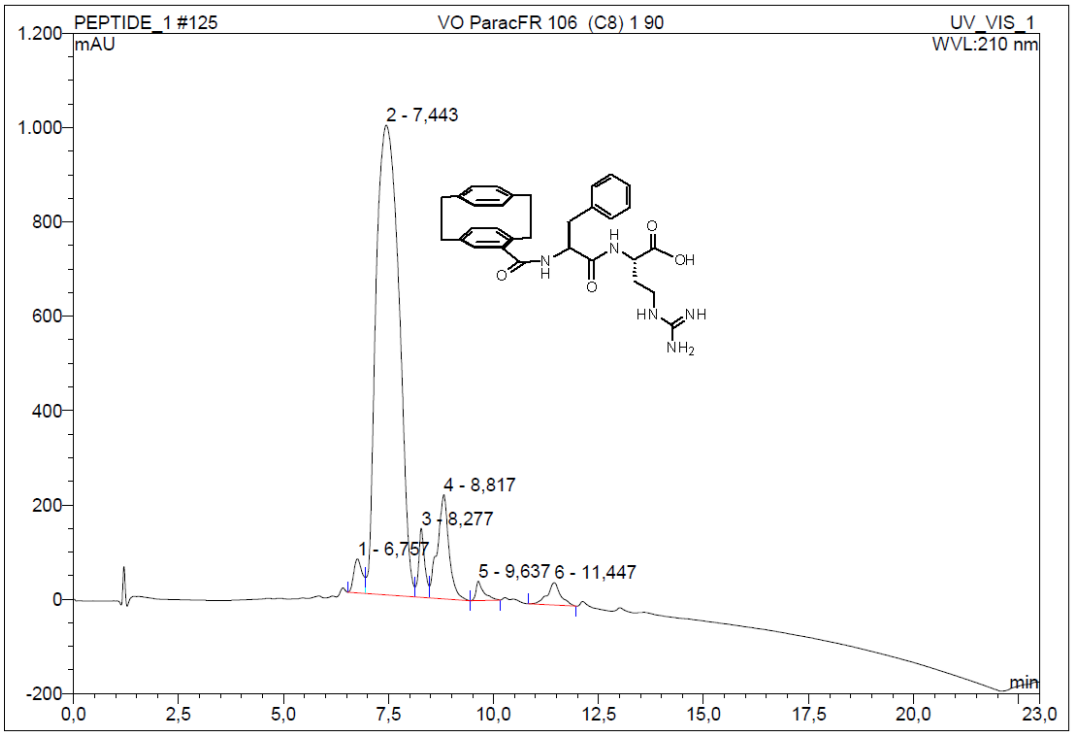

Figure B 6. HPLC chromatogram of [2.2] paracyclophanoyl phenylalanine arginine (**18**).

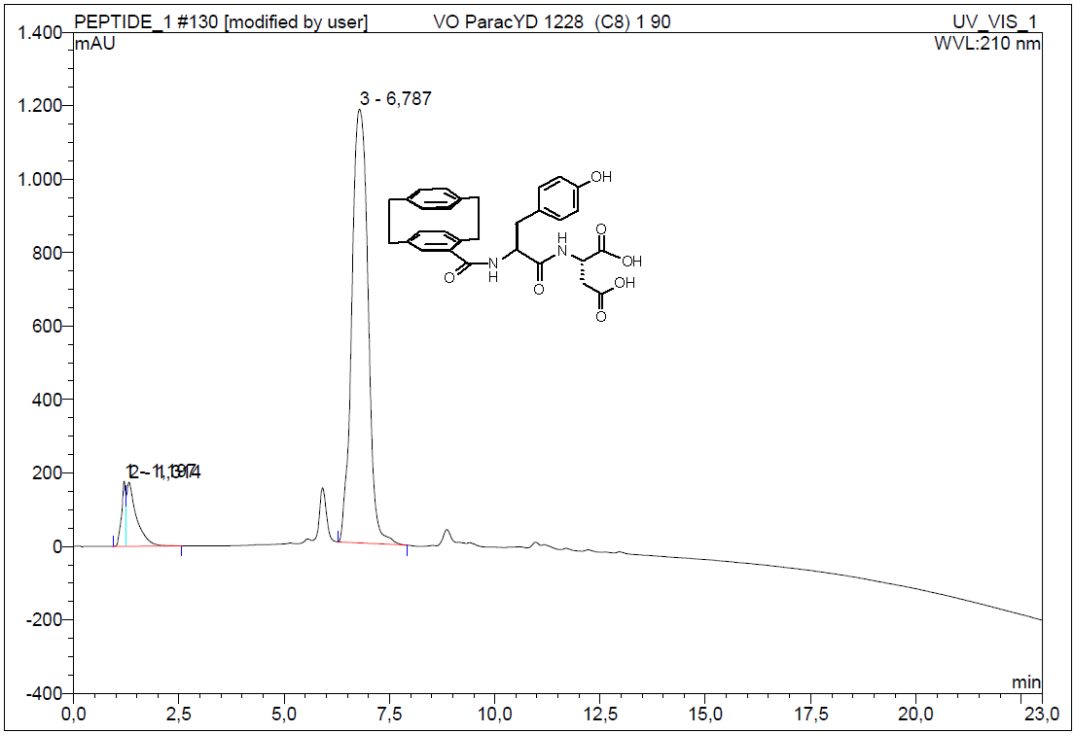

Figure B 7. HPLC chromatogram of [2.2] paracyclophanoyl tyrosine aspartic acid (**19**).

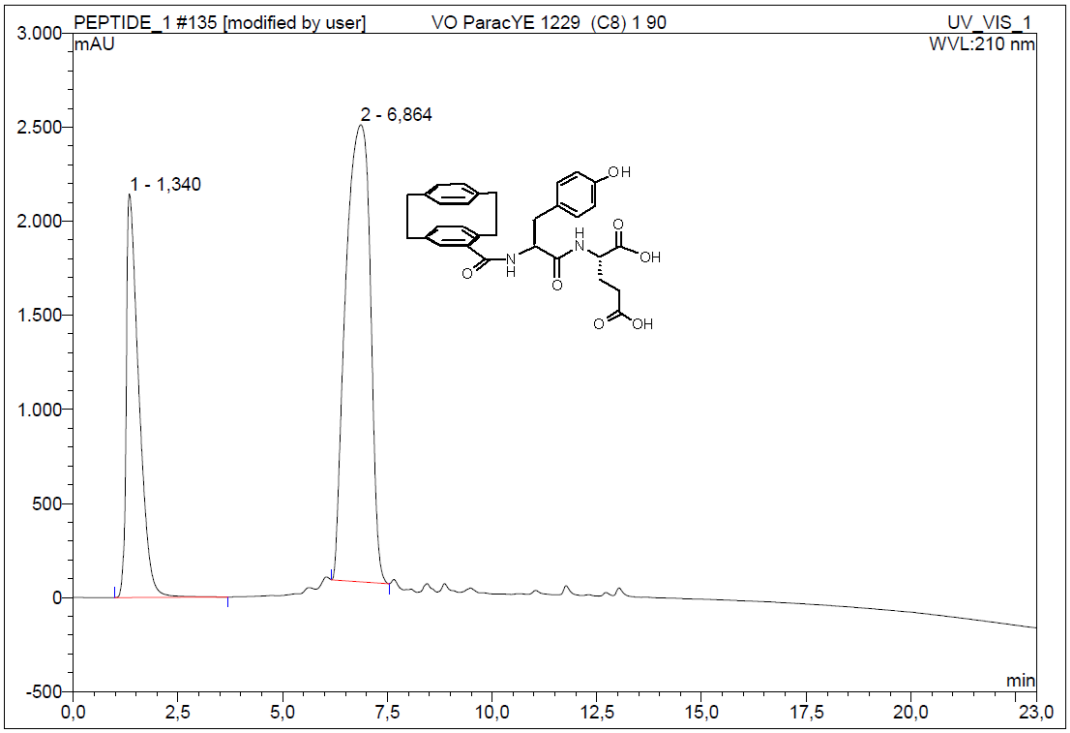

Figure B 8. HPLC chromatogram of [2.2] paracyclophanoyl tyrosine glutamic acid (**20**).

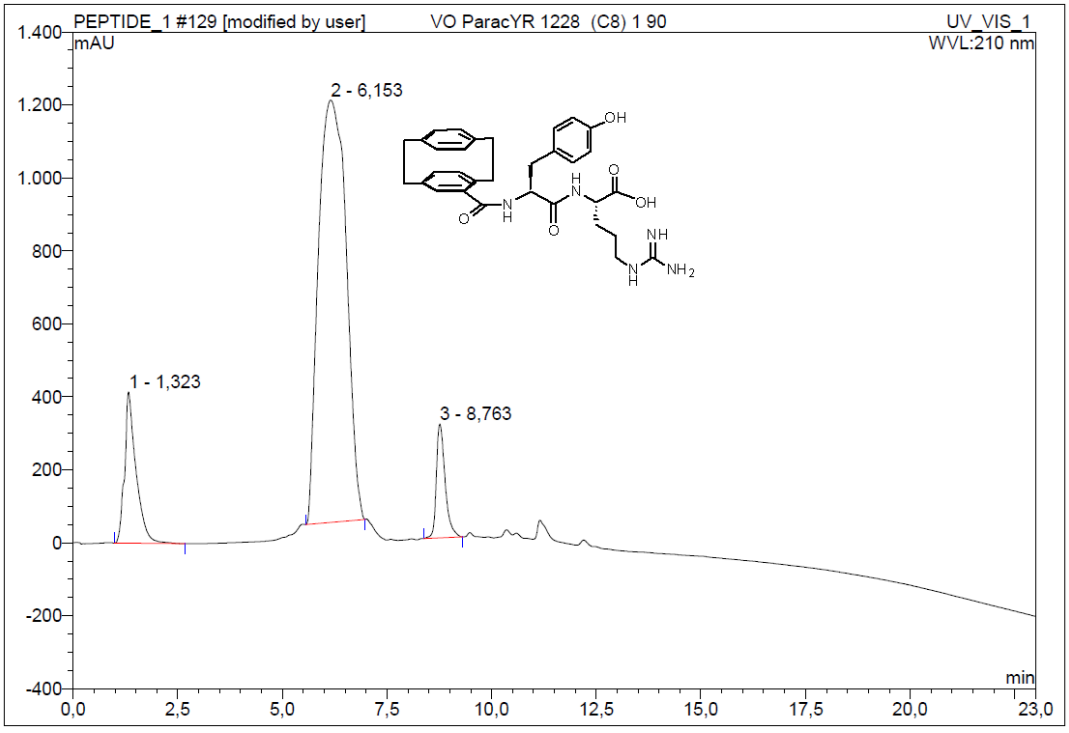

Figure B 9. HPLC chromatogram of [2.2] paracyclophanoyl tyrosine arginine (**21**).

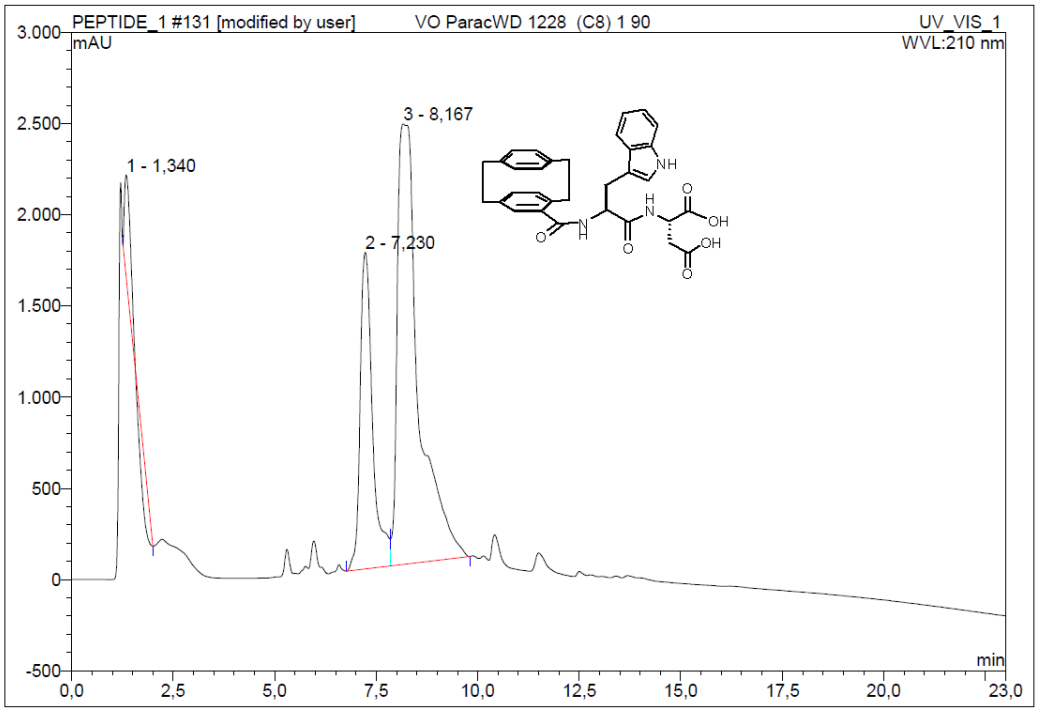

Figure B 10. HPLC chromatogram of [2.2] paracyclophanoyl tryptophan aspartic acid (**22**).

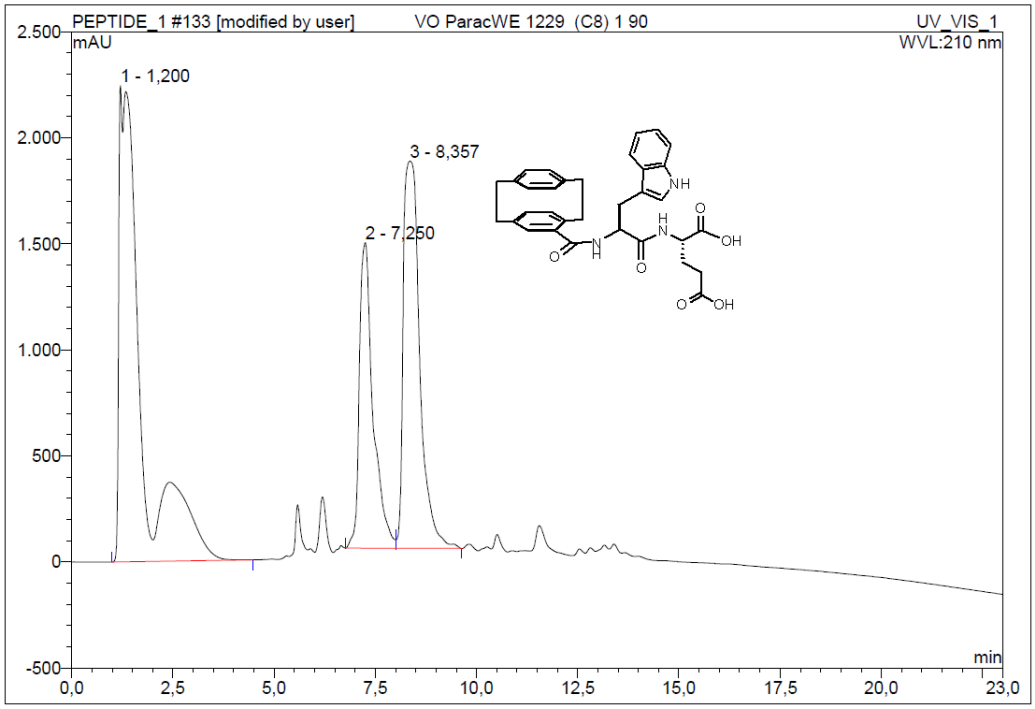

Figure B 11. HPLC chromatogram of [2.2] paracyclophanoyl tryptophan glutamic acid (**23**).

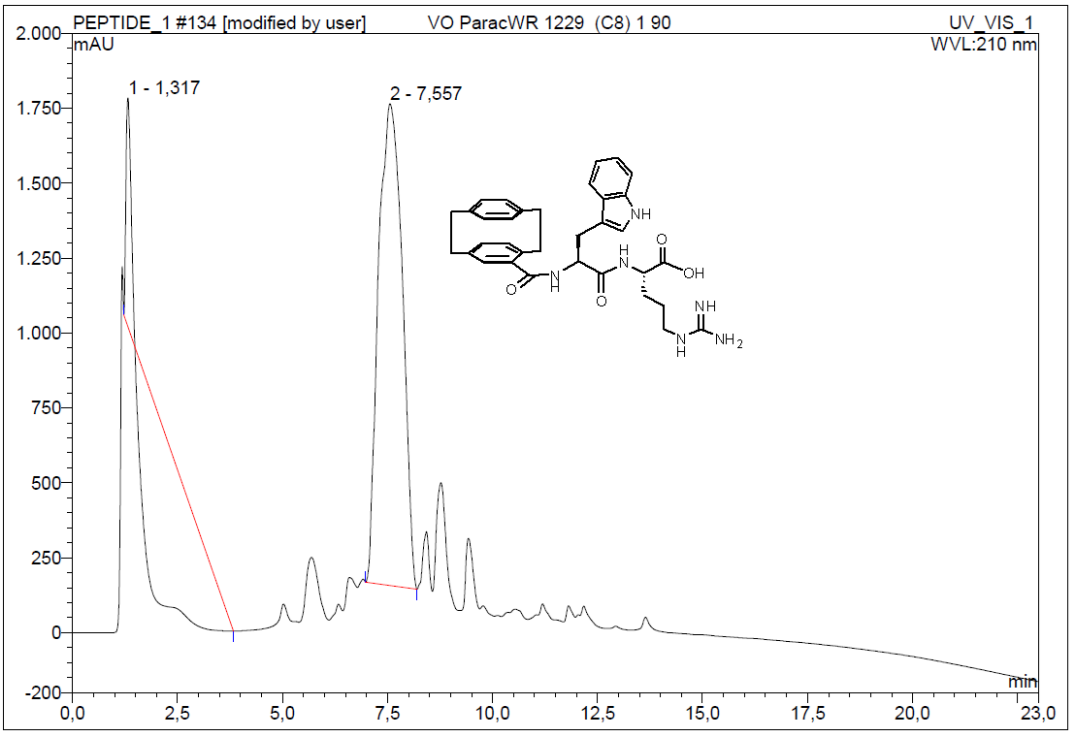

Figure B 12. HPLC chromatogram of [2.2] paracyclophanoyl tryptophan arginine (**24**).

APPENDIX C

HRMS DATA

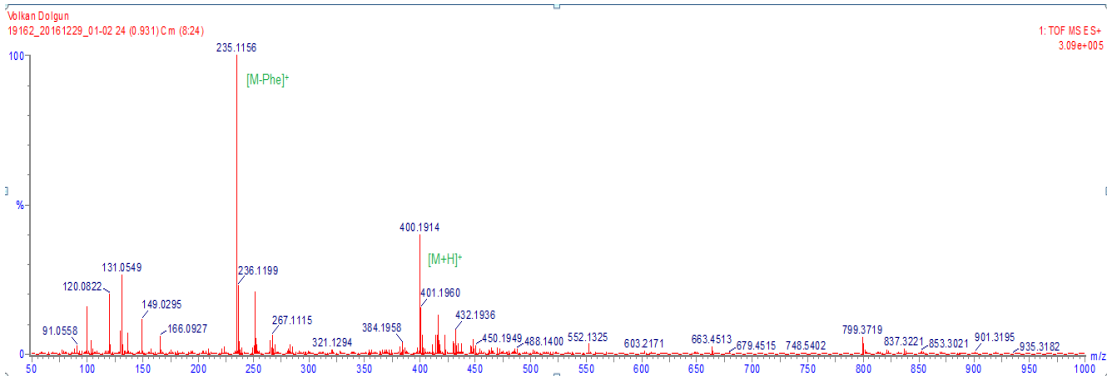

Figure C 1. HRMS chromatogram of [2.2] paracyclophanoyl phenylalanine (**11**).

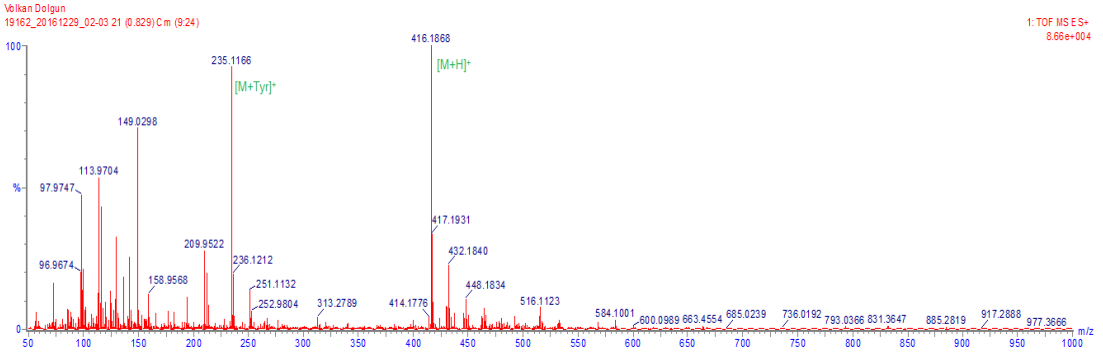

Figure C 2. HRMS chromatogram of [2.2] paracyclophanoyl tyrosine (**14**).

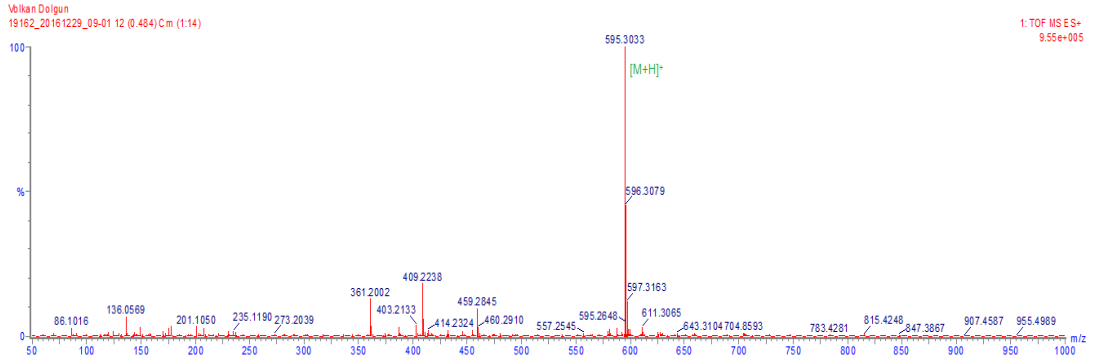

Figure C 3. HRMS chromatogram of [2.2] paracyclophanoyl tryptophan (**15**).

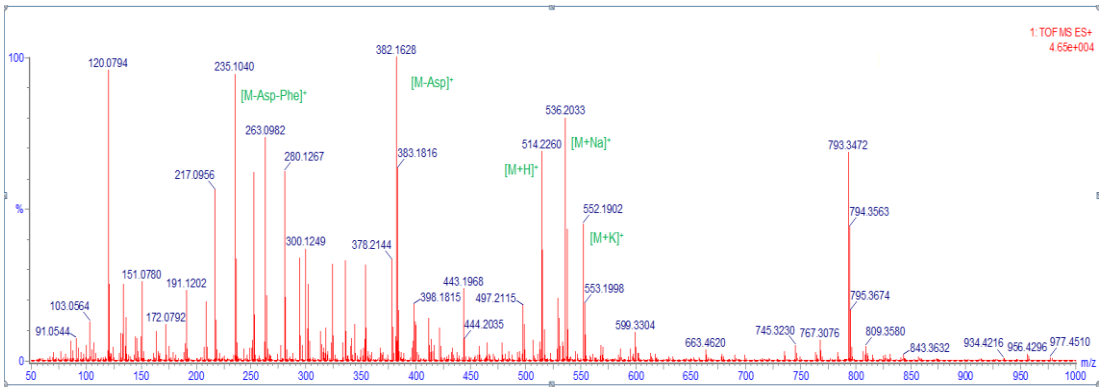

Figure C 4. HRMS chromatogram of [2.2] paracyclophanoyl phenylalanine aspartic acid (**16**).

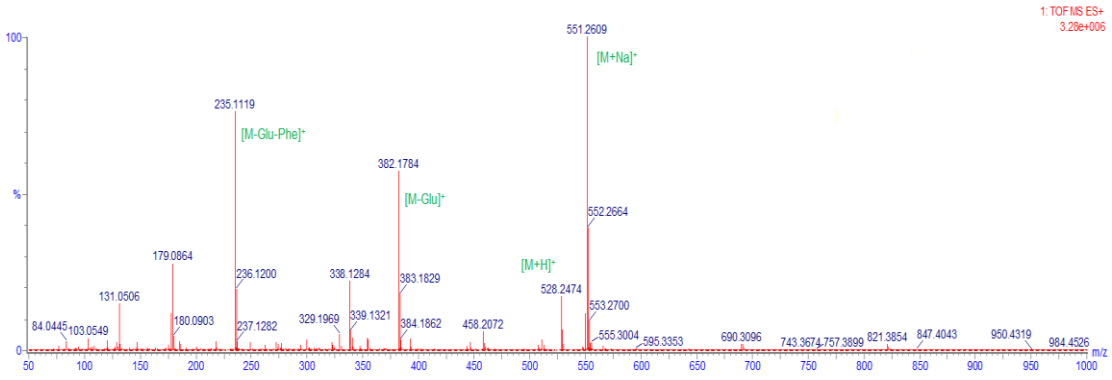

Figure C 5. HRMS chromatogram of [2.2] paracyclophanoyl phenylalanine glutamic acid (**17**).

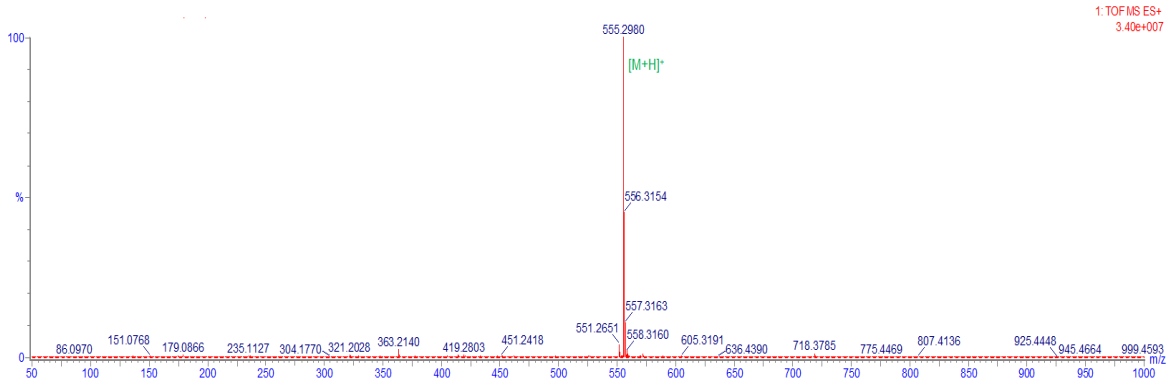

Figure C 6. HRMS chromatogram of [2.2] paracyclophanoyl phenylalanine arginine (**18**).

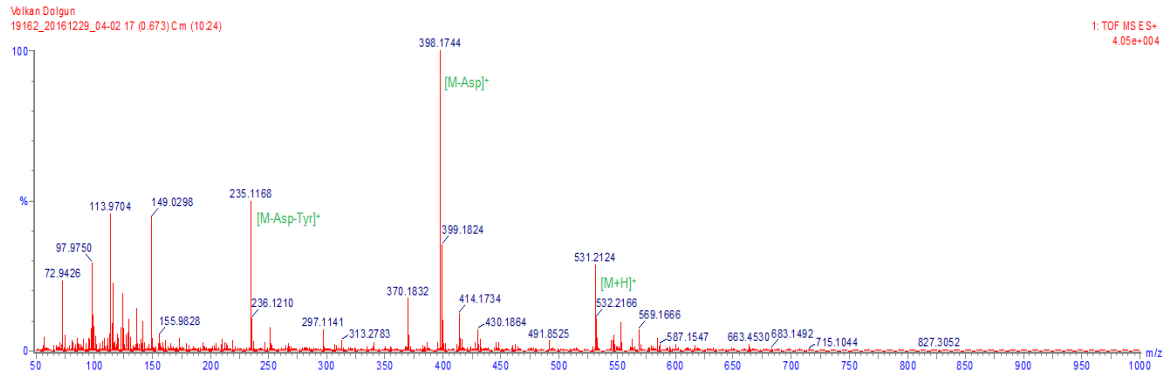

Figure C 7. HRMS chromatogram of [2.2] paracyclophanoyl tyrosine aspartic acid (**19**).

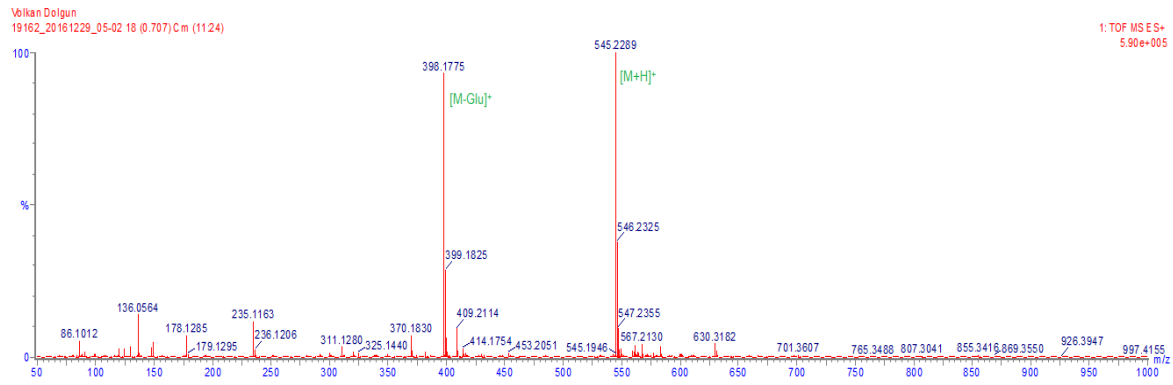

Figure C 8. HRMS chromatogram of [2.2] paracyclophanoyl tyrosine glutamic acid (**20**).

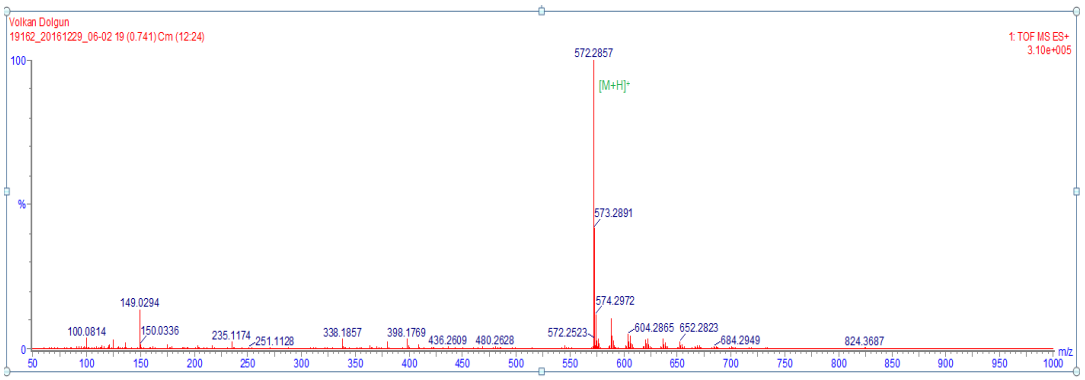

Figure C 9. HRMS chromatogram of [2.2] paracyclophanoyl tryptophan arginine **(21)**.

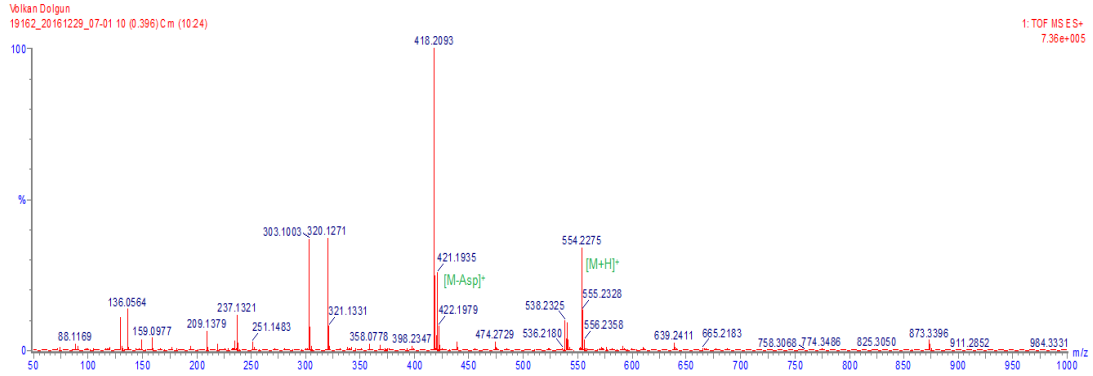

Figure C 10. HRMS chromatogram of [2.2] paracyclophanoyl tryptophan aspartic acid (**22**).

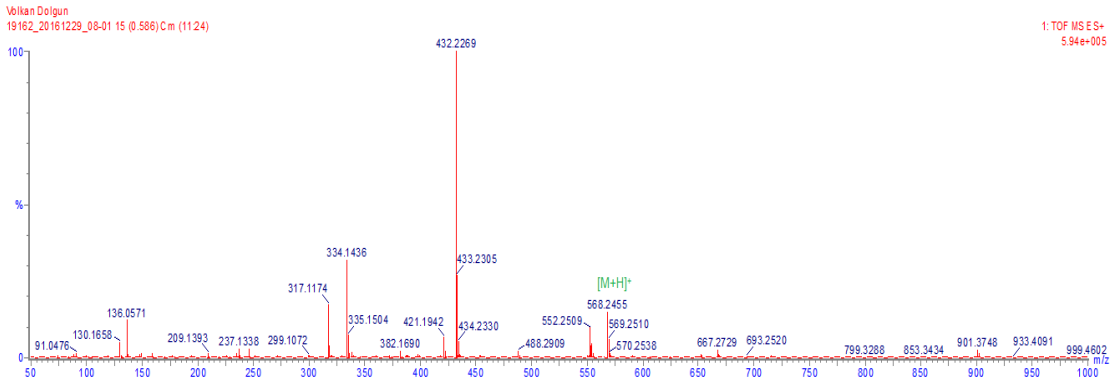

Figure C 11. HRMS chromatogram of [2.2] paracyclophanoyl tryptophan glutamic acid (**23**).

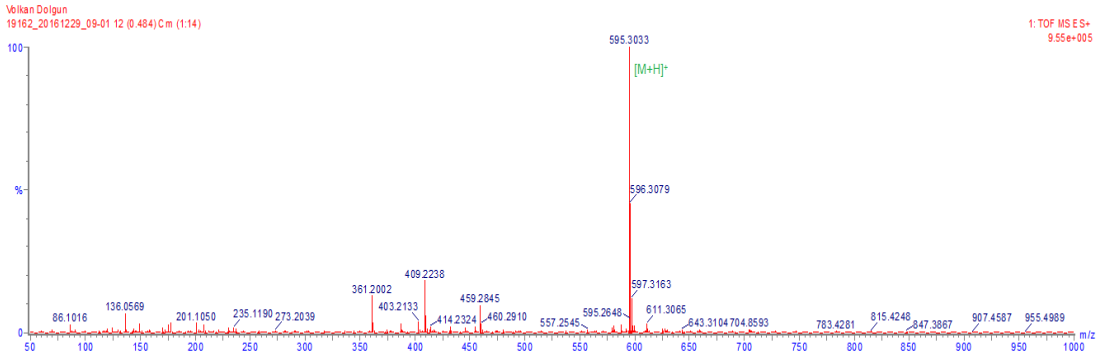

Figure C 12. HRMS chromatogram of [2.2] paracyclophanoyl tryptophan arginine (**24**).